Synthesis and Characterization of Hierarchical EU-1 Zeolite and its Application in Converting Dimethyl Ether to Olefins

BY

Mohamed Hassan Mohamed Ahmed

A Thesis Presented to the

DEANSHIP OF GRADUATE STUDIES

KING FAHD UNIVERSITY OF PETROLEUM & MINERALS

DHAHRAN, SAUDI ARABIA

In Partial Fulfillment of the
Requirements for the Degree of

MASTER OF SCIENCE

In

CHEMICAL ENGINEERING

Dec, 2014

KING FAHD UNIVERSITY OF PETROLEUM & MINERALS

DHAHRAN- 31261, SAUDI ARABIA

DEANSHIP OF GRADUATE STUDIES

This thesis, written by **Mohamed Hassan Mohamed Ahmed** under the direction of his

thesis advisor and approved by his thesis committee, has been presented and accepted by

the Dean of Graduate Studies, in partial fulfillment of the requirements for the degree of

MASTER OF SCIENCE IN CHEMICAL ENGINEERING.

Dr. Mohammed Ba-Shammakh
Department Chairman

Dr. Salam A. Zummo
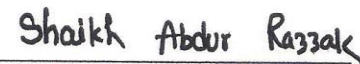Dean of Graduate Studies

30/12/14
Date

Dr. Adnan M. Al-Amer
(Advisor)

Dr. Oki Muraza
(Co-Advisor)

Dr. Mohammad M. Hossain
(Member)

Dr. Zuhair O. Malaibari
(Member)

Dr. Abdur Razzak Shaikh
(Member)

Mohamed Hassan Mohamed Ahmed

2014

DEDICATION

I would like to make special dedication for my parent for their endless support during pursuing

my master studies abroad. Warm feelings of gratefulness go to my sister, who I shared with her

family the best moments during my master studies.

I dedicate my thesis work also to all my family members and all my friends in KFUPM

especially those friends who were my classmate in my undergraduate studies. The dedication

should goes to my close friend and roommate Ahmed, who passed away last year and I pray to

god to forgive him and have mercy upon his soul.

Finally, this research work cannot be done without the support of Dr. Oki Muraza. He was

more than co-advisor to me during this work. He gave me many advices not in the research

only but also in all life. He deserves from me to dedicate this work to his efforts.

ACKNOWLEDGMENTS

TABLE OF CONTENTS

LIST OF TABLES

LIST OF FIGURES

ABSTRACT

Full Name   : Mohamed Hassan Mohamed Ahmed
Thesis Title   : Synthesis and Characterization of Hierarchical EU-1 Zeolite and its
                      Application in Converting Dimethyl Ether to Olefins
Major Field   : CHE
Date of Degree : December, 2014

Hierarchical (or mesoporous) zeolites present one of the promising solutions of the diffusion problem in the catalytic reaction. Creating mesoporous was performed by removing some elements from the zeolite structure either by desilication or dealumination depending on (Si/Al) of the synthesized zeolite. Introduction of mesoporosity into the surface of the zeolite catalyst has many advantages and disadvantages, generally demetalation will increase the surface area and consequently will enhance the mass transfer. On the other hand it will affect the acidity which plays a key role in many reactions and also it will affect thermal stability of the crystals. Developing mesoporosity on the surface of one-dimensional zeolites is still more promising as compared with three-dimensional zeolites because of diffusion limitations. Applying this hierarchical technique on EU-1(EUO) zeolite which has excellent applications in diverse acid-catalyzed reactions, including methanol and dimethyl ether to olefins will improve the conversion and also can be functionalized to improve the selectivity towards a specific valuable products.

The desilicated samples were further treated by nitric acid which called sequential treatment. In the sequential alkaline and acid treatment the best characterization and testing results were observed on EU-1 (0.5,4). Characterization results show promising features for the sequential acid and alkaline treatments on EU-1 zeolite. The mesoporosity increased by 15% for EU-1 (0.5,4) sample as compared with the parent sample, the total acidity also increased from 0.27 to

0.52 mmol/g. The treated samples were evaluated for converting dimethyl ether to olefins. The conversion increased from 37% to 48% together with increasing of propylene selectivity form 11% to 24%.

ملخص الرسالة

الاسم الكامل: محمد حسن محمد أحمد

عنوان الرسالة: تحضير وتشخيص الزيولات الهرمي EU-1 وتطبيقه على تحويل ثنائي ميثايل الايثر

التخصص: هندسة كيميائية

تاريخ الدرجة العلمية: ديسمبر 2014

الزيولات الهرمي أو الزيولات ذو المسامات متوسطه الحجم يعتبر من أحد أهم الحلول الواعدة لمشكلة الانتشارية فى التفاعلات المحفزة. يمكن الحصول علي هذه المسامات متوسطة الحجم بإزالة بعض جزيئات الألمنيوم او السيلكون من البنية الجزئية للزيولات المحضر فى المعمل. وجود هذه المسامات الواسعة علي سطح الزيولات يوفر العديد من المزايا وله بعض السلبيات. فعموما، وجود هذه المسامات يسهل عملية انتشار المواد المتفاعلة والحصول علي المنتجات بسهولة. ولكن فى المقابل بعض الجزيئات فى بنية الزيولات يؤثر علي درجة الحموضية وهي التي تتحكم فى مسار التفاعل كما يؤثر علي الثبات الحراري للزيولات. تطوير هذا النوع من المسامات يعتبر وعاد أكثر بالنسبة للزيولات ذات البعد الاحادي مقارنة بالزيولات ثلاثي الأبعاد. الفكرة من تطبيق هذا العمل فى زيولات EU-1 تأتي من النتائج الممتازة التى أظهرها هذا النوع من الزيولات فى العديد من التفاعلات مثل تفاعل تكسير النافثا وتفاعلات تحويل الميثانول والإيثرات الي أوليفينات وهي منتجات ذات أهمية عالية فى الصناعة.

في هذا البحث تم إزالة بعض جزيئات السيلكون أولا باستخدام محلول هيدروكسيد الصوديوم وبعدها تم إزالة بعض جزيئات الألمنيوم بإستخدام حمض النتريك. العينة التي تم معالجتها 0.5 مولارية من محلول هيدروكسيد الصوديوم متبوعة ب 4 مولارية من حمض النتريك أظهرت أفضل النتائج. تم بنجاح فى هذه العينة زيادة المسامات متوسطة الحجم بمقدار 15% مقارنة بالعينة الأم كما تم أيضا زيادة درجة الحموضة من 0.27 الي 0.52 ملي مول/جرام. بالنسبة لتفاعل تحويل الايثر الي أولفينات تم زيادة نسبة التحويل من 37 الي 48% كما تم زيادة إنتاجية البروبالين من 11 الي 24% .

CHAPTER 1

INTRODUCTION

1.1 EUO (EU-1) framework topology

EU-1 (EUO) zeolite is one-dimensional channel system and the research in this type of zeolite is still more interesting because EU-1 has many applications in important reactions like parafins cracking, methanol and dimethyl ether to olefins and isomerization of C8 aromatics. EU-1 has 10-MR opening running along the direction connected to 12-MR side pockets in the (001) direction. The 10-MR channels are confined but the 12-MR side pockets are more accessible with the dimension of 6.8 x 5.8 A [1].
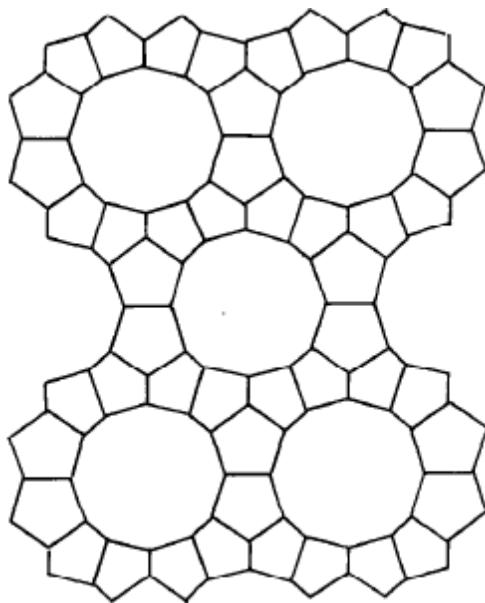
Figure 1: Framework structure of EUO zeolite [2]

Careful studies of synthesis parameters are required as different zeolitic phases can be produced from the same template which is hexamethonium bromide [3-7]. The possibility to get impurities during the synthesis is large as the synthesis is very sensitive to temperature change, synthesis time and aging time. Giordano et al. reported the effect of Si/Al ratio, Si/template ratio and Si/OH$^-$ ratio on EU-1 synthesis [3]. We used the optimum ratio of those parameters as the starting point to study the aging time, synthesis time and crystallization time.

1.2 Hierarchical structure for one-dimensional zeolites

The diffusion limitation is still the major issue that affecting the catalytic performance of one-dimensional zeolites [8-11]. Nanosized zeolites are presenting one of the possible solutions to overcome the diffusion restriction [12-15]. However, during the synthesis stage of the zeolite crystals, the agglomeration takes place and thus eliminates accessing and diffusion to many isolated crystals inside the particle [14-16]. Consequently, the nanosized zeolite alone does not present the complete solution to the diffusion limitation. Combining between the solution of nanosized zeolite and the hierarchical structure is presenting very good idea toward more elimination of diffusion problem. Moreover, the hierarchical structure will give the chance for more selectivity toward specific products [17-23]. This property can be functionalized to produce valuable petrochemicals products such as propylene which has large market demand.

Practically there are two procedures to enhance the mass transfer in the zeolite crystal and to prevent and suppress zeolite deactivation. The first procedure is to reduce the length of the diffusion path, these type of nanosized or nanocrystals structure have been already achieved for some types of zeolite structure, but there are some limitations for this solution which are the

recovery from synthesis solution and the handling way is also difficult [24-26], plus some difficulties inside the packed bed reactor because of pressure drop a cross the column.

The second procedure to enhance the mass transfer is by coupling microporosity together mesoporosity in the external surface of zeolite, and that noticed to give many important advantages because existence of mesoporous on the surface which facilitates accessing to inside microporous which hold the active site and as a result it will increase the zeolite activity and will have more surface area for reaction [27, 28]. In addition, having much mesoporous on the external surface will reduce or prevent the blocking of the pores specially in the case of cracking reaction because the pores in this case are large enough so it will increase the life time of the zeolite [28, 29]. So generally in the case of hierarchical zeolite both the reactants and the products will have easy going in and moving out from the pores or in other words introducing of mesoporous will enhance the mass transfer. But the main disadvantage of this hierarchical structure is that it will yield to decrease the thermal stability of the zeolite [30, 31].

There are two main approaches to synthesis hierarchical zeolite either by template-synthesis or post-synthesis approach. The template-synthesis approach depends on having an organic material that can offer the existence of mesopores and micropores together in its structure [32, 33], so the synthesized zeolite will have the same structure. Actually there are few organic materials which have this property and the common known one is carbon nanotubes (CNT), but the limitation of using these materials is coming from the expensive price and cannot be recyclable after the synthesis [34, 35].

The selection of appropriate Si/Al ratio is very important to create the mesoporosity [36-38], zeolites with too low Si/Al ratio will not give mesoporosity after treatment because it is so difficult to extract the Si atoms from the structure. In the other case, when the Si/Al ratio is too

high, desilication will end up with the dissolution of the zeolite. In the literature, it has been found that the optimum Si/Al to achieve good desilication and mesoporosity is between 25-50 [10], and in our case here EU-1 zeolite crystals with Si/Al of 25 have been used.

The major challenges of introducing mesoporosity on the zeolite surface are controlling the size and the depth of these mesopores introduced and the regular distribution of the mesopores all over the surface. Actually it has been found that treatment parameters like concentration of alkaline can be optimized to achieve the required size of mesopore, for the case of mesopores distribution stirring and treatment temperature are important parameters but still they are not enough to overcome this problem.

1.3 Selective conversion of dimethyl ether to olefins

The market demand of light olefins is increasing rapidly because they are major raw material source of petrochemicals industry [39]. The availability of other cheap materials like methanol which can be converted to valuable olefins by using functionalized catalysts is very interesting research topic nowadays. The reaction of methanol to olefins over solid-acid catalyst passing throws dimethyl ether (DME) and water as intermediate products. It has been found that if we separate this reaction into two steps reaction (methanol to DME and DME to olefins) it will increase the total conversion because each reaction required specific conditions in term of acidity and crystal size.

Utilizing syngas to produce light olefins is taking more attention in the research community. One of the old procedures developed and applied was to produce methanol from syngas as first step and then converting methanol to light olefins as second step. As we mentioned before this reaction will pass throw DME and water as intermediate products. The following equation is describing the steps of this reaction:

4

$$2CO + 4H_2 \rightleftharpoons 2CH_3OH \rightleftharpoons CH_3OCH_3 + H_2O$$
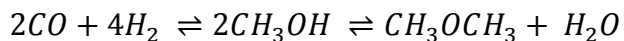
Current researches focus on the elimination of water from the overall reaction. The elimination done by avoiding the producing of methanol .Therefor, the other alternative and promising procedure to produce olefins from syngas is to produce DME directly and then converting the DME to olefins. The stoichiometric equation for this reaction as follows:

$$3CO + 3H_2 \rightarrow CH_3OCH_3 + CO_2$$
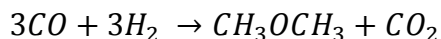
The DME to olefins procedure (DTO) is considered much better than methanol to olefins. Many reasons can attribute to this conclusion and one of the major reasons is lowering of the equipment costs [40-42]. Using the methanol procedure is required to separate the unreacted methanol, DME and the produced water. Therefore, this will make many difficulties related to manufacturing and operation conditions [43-45]. The economic considerations are also taking place because of the higher selectivity of DME to hydrocarbon as compared with methanol conversion. The homogeneity of the reactant and the product (both are hydrocarbons) in the case of DME make the selectivity higher by 38% over when using DME instead of methanol [46]. Actually, searching for suitable catalysts for the DME to olefins reaction is very important step because the possibility of conversion of light olefins to form paraffins, aromatics, naphthenes and higher olefins by hydrogen transfer, alkylation and poly-condensation is very high [47]. Selective conversion of dimethyl ether to olefins (especially propylene) which has great market demand and thus became hot research topic. EU-1 zeolite showed high conversion of methanol to olefins in previous work [48, 49]. As reported also, the MTO reaction passing throws DME as an intermediate product together with water [49], then the DME converted to light olefins. Also for similar work of SAPO-34 (a 3-D zeolite), hierarchical structure of SAPO-34 gave higher

selectivity toward propylene compared with the parent sample [34]. Therefore, the good catalytic results of EU-1 for methanol to olefins are expected to be achieved again in DME to olefins.

Moreover, the DME reaction is releasing less heat than the methanol reaction. Previous works showed the amount of heat ejected is 70% less in the case of DME [50]. They explained that by the elimination of dehydration reaction (conversion of methanol to DME and water) which is the reason of releasing large amount of heat. This advantage of DTO over MTO will increase the catalyst stability due to working in lower temperature conditions.

Comparing the two stoichiometric equations of DTO and MTO reaction, the ratio of H_2/CO is 2 in the case of MTO and 1 in the case of DTO. When this ratio is close to 1, this will give many advantages in saving energy and equipements besides the best utilizing of the syngas as a feedstock for DME production [51].

Based on thermodynamics consideration the water gas shift reaction in the case of MTO required to apply high pressure to shift the equilibrium to produce more DME and water. This consideration is eliminated in the case of DTO. Therefore, the operating pressure is much lower in this case together with high conversion of CO reached to 90%. Consequently, working at lower pressure condition will reduce the capital cost of the equipment [46].

In Figure 2. There is a schematic drawing Berty Stationary Basket Catalyst reactor which is now frequently used for the conversion of DME to olefins.

(a)

Reactor Flange
Rubber Gasket
Flange Screw
Reactor Body
Thermocouples
Catalyst Basket
Catalyst Bed
Impeller
Electric Heated Jacket
Inlet Nozzle
Outlet Nozzle
Impeller Shaft
Water Cooled Jacket
Encapsulated Magnetic Assembly
Tachometer Pick-up

(b)
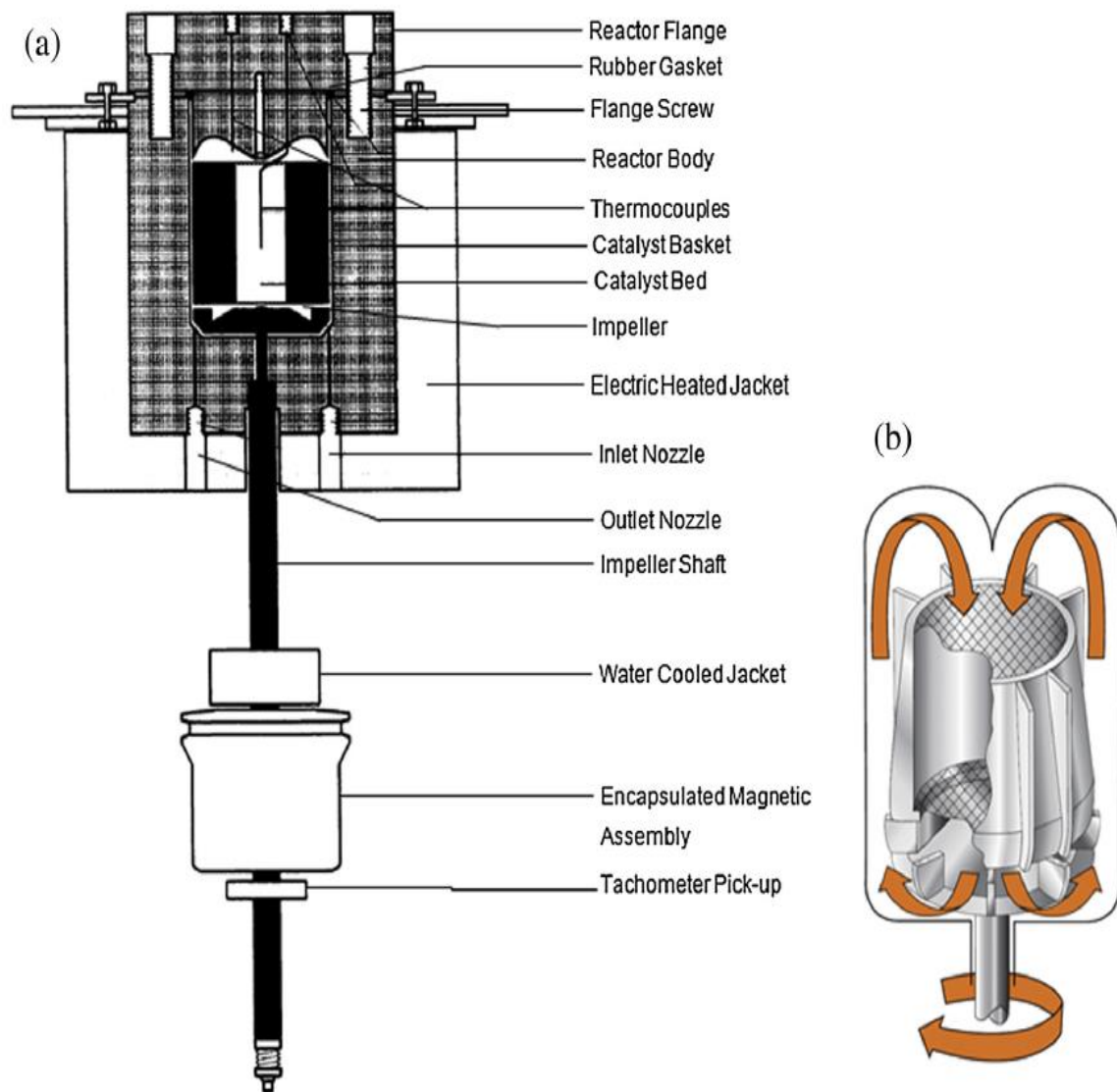
Figure 2 : Schematic drawing for Berty reactor used for DTO (a) detailed assembly. (b) Gas circulation pattern [46]

CHAPTER 2

LITERATURE REVIEW

2.1 Background of EU-1 synthesis

EU-1 (EUO) was firstly synthesized in 1981 by Casci et al. [1] as a new invention. Two different organic materials (OSDA) which are hexamethonium (HM) and dibenzyl-dimethyl ammonium (DBDMA) were used as template for synthesizing EU-1 structure. Most recent research works focus on using of hexamethonium bromide as a template more than other (OSDA) because it's relatively cheap and easy to synthesize material [4-6, 52]. Previous research conduct in 1989 by Rao et al. [5] investigated the effect of the aging time on the EU-1 crystallinity using benzyl dimethylamine and benzyl chloride as templates. They reported the wide effect of aging time on the crystallinity. Recent works in 2009 by Giordano et al. [3] and in 2011 by Xu et al. [6] used hexamethonium bromide as a template for synthesizing EU-1. They investigated two synthesis

Table 1 : Previous works on the effect of synthesis parameters on EU-1 crystals

Parameter	Synthesis condition	Template	Effect of parameters on EU-1 crystals	Ref.
Temperature	160 and 180 ^{o}C	Hexamethonium bromide	Phase purity was affected by temperature. Co-crystalllization of ZSM-48 and EU-1 was observed.	Xu et al. [6]
Synthesis time	7, 9 and 11 days	Hexamethonium bromide	Phase purity and crystallinity were affected by crystallization time. Formation of ZSM-48, cristobalite and quartz were reported.	Giordano et al. [3]
Aging time	25 – 60 h	Bezyl dimethylamine and bezyl chloride	Zeolite crystallinity was affacted by aging time.	Rao et al. [5]

parameters which are time and temperature and their effects on phase purity and crystallinity. Table 1. Summarizes the previous works on EU-1 synthesis parameters. Table 2. Gives the different recipes used for the synthesis of EU-1 zeolite.

Table 2 : Different recipes used in literature to synthesis EU-1 zeolite

	Precursor composition					(SiO$_2$)	(Al$_2$O$_3$)	t (h)	T (°C)	Heating Mode
	SiO$_2$	Al$_2$O$_3$	Na$_2$O	HMBr	H$_2$O					
1	86.8%	5.1%	8.1%		3200	Microsil Silica	Sodium aluminate	1	97	Autoclave [5]
2	97.2-99.5%	0.29-2.72%	0.02-0.08%						110	[53]
3	83.3-91.8%	2.7-0.46%	7.6-13.8%		10%	colloidal silicasol	sodium aluminate	110-53	120	Oven [54]
4	78.9%	1.3%	3.3-13.1%		3000	fumed silica (Cab-O-Sil M5)	aluminum hydroxide gel	120	90	Autoclave [55]
5	1	1/r*	0.08-0.12	0.01-0.08	30	grade colloid silica	Sodium aluminates	(12)-60	160-180	Autoclave [6]
6	60	1.50	2	6	36-150	Amorphous mesoporous silica extrudates	sodium aluminate	up to 168	180	Autoclave [56]
7	81.4	1.00	10.9–18.6	2.2–11.0		silica sol	sodium aluminate	up to 168	180	Autoclave [57]
8	5.0-75	0.50	3.0-12	2.5-20	3000	fumed silica	aluminium hydroxide	24-264	190	Autoclave [3]

2.2 Alkaline treatment

Actually most of the treatments were done by applying desilication only but some works were reported applying the desilication together with dealumination. The majority type of zeolites is given good results in terms of surface area and active site when they treated with alkaline solutions only and these zeolites are manly have 3D structure framework.

Groen et al. in 2004 [58] applied the only alkaline treatment on ZSM-5 (Si/Al = 17, 37 and 174) by using NaOH. They optimized the treatment parameters (treatment time, base concentration and treatment temperature), they got very large increases in the total surface area of zeolite ZSM-5. In 2004 also same group [59] worked on three types of zeolite (MOR, FER and Beta) by treating with NaOH only and they controlled the size of mesopores by varying treatment time and temperature and also the reported changing on surface area and zeolite acidity.

In 2008 Groen et al. [60] treated zeolite BEA (Si/Al = 35) with NaOH and they optimized two treatment parameters (treatment time and temperature), they also reported the sever decreases in the micropore volume of the alkaline-treated samples and they suggested to lowing the temperature and shorting the time of the treatment to suppress these effects.

In 2009 Bonilla et al. did a particular study for desilication of ferrierite zeolite (Si/Al = 29) using NaOH [61]. They did a comparison between dealumination and desilication efficiency on creating mesopores. They reported that the desilication is more efficient 3 to 4 times than dealumination in that. They also told about the importance of treatment conditions (time of treatment, NaOH concentration and temperature) on the quality of the created pores in terms of

size and distribution. Unlike other zeolite frameworks (MFI, MTW, MOR, and BEA, ferrierite zeolite required relatively high concentration treatment to extract the Si species from the structure. The assessment for the desilicated samples was performed on catalytic pyrolysis of low-density polyethylene. The performance of treated samples was higher than the parent and the distribution of the product was wider. They highlighted the point of harsh treatment and its bad effect of the crystal structure which consequently, reduce the catalytic activity of the zeolite.

Different types of 3-D framework were investigated. In 2010, SSZ-13 (Si/Al= 15) which is CHA framework was desilicated with different NaOH concentrations [62]. Unlike MFI topology, the desilication process led to decrease in internal surface area and the crystallinity. Moreover, Co-adsorption on FT-IR showed decreasing in the total number of Bronsted acid sites but with preservation on its strength. The methanol to olefins (MTO) reaction used to test the activity of the desilicated and the parent sample. Consistently with the surface area and acidity results, the desilicated samples showed lower catalytic activity in converting methanol. More than that, the life time was shorter as compared with parent sample. The only advantage reported for this treatment was in the amount of deposited coke on the outer mesopores which was less than the amount deposited in the micropores in the parent sample.

In 2011 Svelle et al. [63] studied the desilication on ZSM-5 and they used electron microscope and infrared spectroscopy to observe the defects on zeolite morphology and external surface of the crystal, This realization has allowed them to identify a preferred particle morphology for efficient desilication of ZSM-5, they concluded that particles constructed of fused subunits appear to be very susceptible towards directed mesopore formation by desilication.

In 2011 Matias et al. [8] studied the effect of low NaOH concentration on TON zeolite framework (Si/Al = 31), they focused on the effects of this treatment on the porosity, acidity. They tested the samples on butane isomerization reaction. They reported some observations on the TON acidity which was that a limited decrease on the concentration of Brønsted acidity and on the other hand a significant increasing on the concentration of Lewis acidity. On the surface porosity they observed formation of mesopores of around 20 nm sizes. They reported that there was no effect of desilication on zeolite stability.

In 2012 Couto et al. [11] studied the desilication on NU-10 zeolite. They investigated the effects of different NaOH concentrations and treatment times. They observed an increasing in the total microporosity of the treated samples especially in the sever conditions. On the other hand, they reported decreasing in the acidity. They tested the treated sample in o-xylene isomerization and they reported higher activity for the treated samples over the parent one. Generally, they observed improvements in the internal and external diffusion together with shape-selectivity toward specific products.

More work on desilicated ZSM-5 zeolite was performed in 2013 by Li et al. [64] to be evaluated on fast pyrolysis (CFP) of lignocellulosic biomass. They used different concentrations of NaOH (0.1 – 0.5 M) to treat the parent ZSM-5. The performance of the treated samples in selectivity and conversion was based on the concentration of NaOH used for treatment. But in general they reported increasing on the activity and diffusion beside more selectivity toward specific products for treated samples. Regarding the high concentration of NaOH used at 0.5 M,

they observed a considerable decreasing in microporosity which consequently affected the total conversion of lignocellulose to aromatics.

To give more attention to the catalytic applications of hierarchical zeolites especially ZSM-5, a brief study was performed by Bleken in 2013 [65] on the deactivation rate of the desilicated ZSM-5 which was used to convert methanol to hydrocarbons. From the top to the bottom of the reactor different samples of catalysts were characterized to study the formation of coke. The desilicated samples showed a homogenous distribution of coke along the reactor axis. The regeneration process of desilicated catalysts can be performed in a lower temperature condition which gave a chance to save more energy. Finally they reported that the rate of deactivation is too high in the bottom of the reactor than in the top for the desilicated samples.

In a recent paper published in 2014 another type of zeolite which is SVR (Si/Al=40) was investigated in desilication treatment. Shamzy and his team [66] studied the effects of two treatment parameters which are the NaOH concentration and time on the acidity and textural properties of the zeolite. They found that increasing pH of treatment solutions will effect decreasing the micropore volume and Brønsted acid sites, while it will increase the micropores surface area and the concentration of Lewis acid sites. They reported that the pore size distributions were shifted towards to mesopore sizes which are indicating the formation of mesoporosity.

Recent work in 2014 by Tarach et al. [67] on BEA (Si/Al = 22) zeolite treated with NaOH and TBAOH to create mesoporosity. They tested the desilicated samples on fluidize catalytic

cracking of n-decane and 1,3,5-tri-iso-propylbenzene to produce diesel. The performance of the treated samples was higher as compared with parent sample together with observing of more selectivity toward propylene. The characterization results showed uniform formation of intracrystalline mesoporosity when using of NaOH and TBAOH in the treatment.

Continuing the research in other type of zeolites, ZSM-58 was first time studied in 2014 by Biemelt et al [68]. They applied two different processes which are desilication and desilication re-assembly to obtain the hierarchal structure and they used NaOH and NaOH with cetyltrimethylammonium bromide (CTAB) to perform these processes respectively. For the desilication process they reported the increasing of pore volume with the increasing of NaOH concentration. Moreover, they reported the insignificant effect of increasing Si/Al ratio on the number of mesopores created. The other re-assembly process led to highly increasing in the surface area together with narrow size distribution of the mesopores created. Finally, they reported significant decreasing of strong acid site with the increasing of NaOH concentration.

2.3 Sequential alkaline and acid treatment

In 2005 Groen et al. [31] applied the both treatment desilication and dealumination on ZSM-5. They performed the sequential treatment to get porosity modification by alkaline treatment and to tune and control the acidity by steam treatment. The characterization results indicate that the alkaline treatment effect on removing of the Si species together with no significant effect on the acidity. On the other hand, removing the extra-framework Al species by steam treatment led to significant change on the acidity without any evidence of creating of mesopores. They concluded that applying of this procedure in post-treatment can be very useful for controlling the porosity and the acidity.

In 2006, same group [30] did further study on ZSM-5 (MFI) toward more understanding of the sequential alkaline and acid treatment. The research focused on the effect of the position of Al species on the zeolite framework and its effect on creating mesoporosity. It was founded that the suitable and optimum Si/Al ratio to perform alkaline treatment and creating more mesoporosity is 25-50. One of the other important findings of this research was the effect of non-framework Al. The existence of non-framework Al in the structure of the zeolite led to deposition of these Al species on the pore mouth after the alkaline treatment. Consequently, this will effect on the surface area and the acidity of the treated samples. They also focused on the importance of using different time of treatment and acid concentrations in order to optimize the created mesoporosity.

Different framework which is ferrierite (FER) was studied by Verboekend et al. in 2010 [69]. A deeply characteristic research was performed on applying the sequential alkaline (NaOH and NaAlO$_2$) and acid (HCl) treatments. Similar to previous works the deposition of Si and Al

species on the outer surface took place after the desilication. Therefore, the acid treatment recovered most of the blocked micro and mesoporosity. They performed also a comparison between desilication using NaOH or NaAlO$_2$ and their effect on the created mesopores. They assessed the treated samples on pyrolysis of low-density polyethylene reaction and they reported the increasing of the activity of treated samples over the parent one.

In 2010 Van Laak et al. [10] did a comparison between applying desilication only or applying the both treatment together for two types of zeolites which are mordenite and beta. They reported that applying the both treatments together will preserve zeolite crystallinity and will keep Si/Al ratio close to the parent sample, they also reported very large increases in the surface area. They selected liquid-phase alkylation of benzene with propylene to study the catalytic performance of the enhanced accessibility of various mordenite samples, they observed that the activity of treated samples was better than untreated one and the selectivity towards the desired products was higher for treated samples.

In 2011 again TON was studied by Verboekend et al. on ZSM-22 [70]. They told about the difficulties of demetalation because of the structure which is rod-like morphology of the crystal and the small size of the pore mouth. These small pore mouths have been blocked by Al species and this yielded to large decreases in the micropore volume. They suggested doing acid treatment with HCl to remove the Al atoms. The acid treatment successfully recovered 90% of the micropore volume but on the other hand it just recovers 37% of the Brønsted acidity. They concluded that the desilication efficiency of ZSM-22 is relatively low comparing with other

reported types of zeolite like ZSM-5 and ferrierite because of crystal morphology, but it still new promising techniques to do deslication for these types of zeolite.

Another comparison was performed by Qin et al. in 2011 in zeolite Y [71]. The comparison applied between doing dealumination only by ammonium hexafluorosilicate (AHFS) and doing desilication first by NaOH followed by dealumination by ammonium hexafluorosilicate. The results showed that AHFS dealumination led to deposition of Si species on the outer surface which affected in lowing the surface area and the acidity. On the other hand, the sequential alkaline and acid treatment was very effective to create homogeneous aluminum–silicon distribution and much mesoporosity. The parent, desilicated and sequential treated samples were evaluated in 1,3,5-triisopropylbenzene cracking and cumene conversion. The best results were reported for the sequential treated samples in terms of higher conversion and long life time on stream.

New zeolites framework was investigated by Verboekend et al. in 2012. Zeolites Y and USY [72] treated by NaOH base followed by H_4EDTA and Na_2H_2EDTA acids to create hierarchical structure. They reported that low framework density and low Al content were very crucial parameters to create mesoporosity via alkaline treatment. Moreover, they observed the ability of sequential alkaline and acid treatment to remove the amorphous aluminosilicate species for the outer surfer which will increase the zeolite crystallinity. The evaluation results of alkylation of toluene with benzyl alcohol over the treated samples emphasized the importance of optimizing the treatment conditions in order to get better performance in the testing stage.

18

2.4 Another field of application of hierarchical zeolites

In 2011 Wang et al. [9] opened new field for the application of hierarchical zeolites in the area of bioenergy, they synthesized hierarchical zeolite by many techniques post-treatment, hard templating and soft templating, they summarized their results by observing that the mesopores which created by post-treatment were random and uncontrollable in both size and distribution but it is practical way to do that but it will resulted in large change in zeolite crystallinity and acidity, also they observed that few types of zeolites are suitable as parent zeolites for dealumination or desilication. For the case of hard templating by carbon atoms they mentioned that it was not practical technique because of its high cost. In soft templating by using surfactant-based materials, they reported that it is promising technique because it's easy and high productive and also because these materials are cheap. The main target of their research was the broad applications in biomass conversion and biofuels upgrading.

The most interesting works in the literature on hierarchical zeolites have been summarized in Table 3.

Table 3 : Summary of literature works on alkaline and sequential treatments for different types of zeolite frameworks

Zeolite type	Investigator	Year	Si/Al	Procedure	Application	Comments
ZSM-5, MFI	Groen et al	2004	37	NaOH	No application	Increment in surface area
	Groen et al	2005	17 37 176	NaOH+ steam treatment	No application	post-treatment is very useful for controlling the porosity and the acidity
	Groen et al	2006	NA	Alkaline + Acid treatment	No application	The effect of deposited non-framework Al on the surface area. Optimum Si/Al ratio for treatment is 25-50
	Svelle et al	2011	50	NaOH	No application	Defects on zeolite morphology and external surface
	Li et al	2013	50	NaOH	Pyrolysis (CFP) of lignocellulosic	Increment on the activity
	Bleken et al	2013	50	NaOH	methanol to hydrocarbons	Homogenous distribution of coke
FER	Groen et al	2004	27	NaOH	No application	Controlling the mesopre size by varying treatment conditions.
	Bonilla et al	2009	29	NH_4NO_3+HCL	Pyrolysis of polyethylene	Effect of harsh treatment on the crystallinity and the catalytic activity
	Verboekend et al	2010	27	$NaAlO_2$, HCl, and NaOH	Pyrolysis of polyethylene	Increasing of the activity of treated samples over the parent one.
	Sommer et al	2010	14	NaOH	Methanol to olefins	Lower catalytic activity of the treated samples due to pore blocking.
MOR	Jong et al	2010	10	NH_4NO_3 + HNO_3	Alkylation of benzene with propylene to cumene	Better catalytic performance and higher selectivity toward cumene for the treated samples
	Kubu et al	2014	40	NaOH and TPAOH	No application	Increasing pH of treatment solution will affect on decrease the micropore volume and Brønsted acid sites
TON	Groen et al	2004	45	NaOH	No application	Controlling the mesopre size by varying treatment conditions.

Zeolite type	Investigator	Year	Si/Al	Procedure	Application	Comments
SVR	Couto et al	2012	33	NaOH	o-xylene isomerization	Improvement in the activity and selectivity of the treated samples
NU-10, TON	Verboekend et al	2011	46	NaOH+ HCl	No application	The acid treatment successfully recovered 90% of the micropore volume but it just recovers 37% of the Brønsted acidity.
ZSM-22, TON	Biemelt et al	2014	50	NaOH + CTAB	No application	The re-assembly process led to high increasing in the surface area together with narrow size distribution of the mesopores created
ZSM-58, DDR	Verboekend et al	2012	2.4 2.6	NaOH + H_4EDTA and Na2H2EDTA	Alkylation of toluene with benzyl alcohol	Low framework density and low Al content are very crucial parameters to create mesoporosity via alkaline treatment
BEA	Groen et al	2008	35	NaOH	No application	Observing the sever decreasing in the micropore volume of the alkaline-treated samples
	Tarach et al	2014	22	NaOH +TBAOH	Cracking of of n-decane and 1,3,5-tri-iso-propylbenzene to produce diesel	Higher catalytic cracking of the treated samples and more selectivity toward propylene
	Matias et al	2011	31	NaOH	Butane isomerization	Limited decrease on Brønsted acidity, significant increase in Lewis acidity and no effect on stability

2.5 Background of DME to olefins reaction

In 1995 Cai et al. [41] proposed a new route to convert syngas to olefins. The necessity for this procedure came from the difficulties of the previous routes which were used before. These old routes were either converting the syngas directly to olefins or passing throw methanol as first step and then converting methanol to olefins. Because of many difficulties which were mentioned in the introduction, Cai and his co-workers thought about a new route which is converting the syngas to dimethyl ether and then to olefins in two steps. Modified SAPO-34 used as a catalyst for this reaction. The reaction results were very good in terms of conversion which reached to 100% and selectivity for ethylene and light alkenes which reached to 60 and 90% respectively. This work opened new fields for more studying of new process which can provide higher conversion and selectivity beside low energy consumption for producing light olefins.

In 2006, Zhao et al. [49] investigated a new zeolite to convert DME to light olefins. ZrO_2 and H_3PO_4 modified H-ZSM-5 catalyst was used. The objective of their research was to enhance the production of propylene over other olefins because of the increases in its market demand. They succeed in increasing the propylene selectivity to 45% of total products. Moreover, they achieved very high P/E ratio which reached to 16. In other words, they succeeded to favor the formation of propylene over ethylene which will give another advantage from economical point of view.

Same group of Zhao et al. performed a study on DME to olefins over modified SAPO-34 zeotype in 2008 [73]. They synthesized and grew SAPO-34 over α-Al_2O_3 support to enhance the diffusion of both reactants and products. They assessed the modified SAPO-34 using fluidized bed reactor and they made a comparison between the modified catalyst and the spray-dried catalyst and the powder catalyst. The results showed that the two methods performed gave

similar results in terms of conversion and selectivity but the advantage was for the modified SAPO-34 because of higher reaction rate observed.

The works on DTO reaction were mainly over SAPO-34 catalyst with different modifications. Later in 2010 Hirota et al. [74] synthesized nano-crystals SAPO-34 in size of 75 nm and compared their performance in DTO and MTO with other large crystals in size of 800 nm. They reported the long life time of the nano-crystals SAPO-34 over the larger crystals. They explained this by the short diffusion path of the nano-crystals which limited the number of blocked pores. They observed that the rate of coke deposition in the two reactions (MTO and DTO) was the same which indicated that the reaction of methanol to DME has no diffusion limitation problem. This paper research focused on the importance of nanozeolites martials for solving the diffusion problems.

Another promising procedure to eliminate the diffusion limitation is hierarchical structure which was applied on SAPO-34 by Cui et al. in 2013 [34]. Hierarchical SAPO-34 catalysts with different size distributions were assessed on converting dimethyl ether to olefins. They reported the extreme ability of the obtained hierarchical structure in selectivity toward olefins. The selectivity reached to 96% which was very high percentage. Moreover, the modified SAPO-34 recorded higher catalytic activity together with better stability on stream. The justifications for these good improvements are the existence of the mesopores on the outer surface which enhanced the mass transfer and facilitated access to more active sites.

CHAPTER 3

EXPERIMENTAL WORK

3.1 Investigation of synthesis parameters

Pure and highly crystalline phase of EU-1 zeolite was synthesized based on the procedure described by Giordano [3, 75]. The molar composition of the prepared gel was 9 Na_2O–10 $HMBr_2$–0.5 Al_2O_3–25 SiO_2–3000 H_2O. The synthesis started by preparing alkaline solution by adding 0.72 g of NaOH to 54 ml of deionized water. $Al(OH)_3$ (0.08 g) was added slowly to the solution as a source of aluminum followed by 3.62 g of hexamethonuim bromide as an organic structure directing agent. After the solution became homogeneous 1.05 g of fumed silica was added as a source of silica. The above gel was prepared at room temperature and stirring speed of 500 rpm. After 12 h aging time the gel transferred to 100 ml PTFE autoclave and moved to conventional oven at 190 ^{o}C for 72 h. The autoclave reactor quenched in a cold water to vanish the reaction quickly. The produced solids recovered by centrifugation and washed several times by deionized water to normalize the pH. The wet solids transfer to 105 ^{o}C oven for drying overnight. The sample was then calcined at 550 ^{o}C for 12 h to remove the template. The N-EU-1 was converted to NH4-EU-1 by an ion exchange with 2M of ammonium nitrate (NH_4NO_3) for 50 min in a microwave oven. The H-EU-1 was obtained by calcination at 550 ^{o}C for 12 h.

3.1.1 Aging time

The most important parameter affecting the zeolite crystallinity is the aging time [76]. The aging time has been changed from 3 to 24 h to achieve high crystallinity, so the EU-1 zeolite has been synthesized 4 times following the same recipe but with different aging time.

3.1.2 Synthesis temperature and crystallization time

In order to study the effect of temperature on the zeolite crystallinity and morphology the same procedure has been used but at different synthesis temperature (185 ^{o}C and 195 ^{o}C) and different crystallization time 24, 48 and 72 h [77].

3.2 Alkaline treatment

Sodium hydroxide (NaOH) was selected to be the alkaline for the desilication treatment. The synthesized zeolite at 12 h aging time treated with NaOH. The effect of NaOH concentration on the zeolite investigated by using three different NaOH concentrations (0.25, 0.5 and 1 Molarity). The second crucial parameter is desilication time. The desilication contact time was varied at different periods (15, 30 and 60 min).

The treatment was carried out by adding 1 g the zeolite sample to 60 ml of NaOH solution while stirred at 400 rpm in 80 ^{o}C using a hot-plate. After treatment, the samples were washed several times until the neutral pH was obtained. Finally, the catalysts were dried at 105 ^{o}C for 12 h.

3.3 Sequential alkaline and acid treatment

3.3.1 Alkaline treatment

Solutions of different concentrations (0.25, 0.5 and 0.75 M) of NaOH prepared to extract the Si species from EU-1 zeolite structure. 1 g of synthesized EU-1 crystals added to 60 ml of the alkaline solution at 80 ^{o}C at stirring rate of 500 rpm. After 60 min the solution cooled by cold water and the solids separated from the alkaline solution by centrifuge. The solids washed many times and then moved to an oven at 105 ^{o}C for 12 h.

3.3.2 Acid treatment

The desilicated samples again treated with different concentrations of HNO_3 (1, 2 and 4 M). The recovered powder from alkaline treatment was added to 60 ml of HNO_3 solution heated to 70 ^{o}C at 500 rpm stirring rate for 30 min. The solids separated, washed with deionized water and then dried at 105 ^{o}C for 12 h.

3.4 Catalytic evaluation

Fixed-bed reactor used to perform the DME reaction of EU-1 (EUO) zeolite. The reactor made of quartz glass (i.d. 4 mm) with a continuous-flow system under atmospheric pressure. The reaction performed at 350 ^{o}C and the amount of catalyst used was 0.05 g. DME was fed to the reactor with rate of 1.3 mmol/h carried by He gas of rate of 19 mmol/h. The contact time (W/F) was 0.039 kg h /mol. Shimazu GC-14B gas chromatograph was used to analyze the products.

CHAPTER 4

CHARACTERIZATION

4.1 X-ray diffractomoter (XRD)

Miniflex, Rigaku diffracometer was used to analyze the phase and the crystallinity of the powder synthesized. The diffractometer using Cu Kα radiation of (1.5405 Å). The analysis performed in the range of 5 to 50° of 2θ with scan step of 0.02° and a counting time of 4 s for each step.

Advanced software was used to obtain and analyze the data from the diffracometer which is PDXL. PDXL provides various analysis tools such as automatic phase identification, quantitative analysis, crystallite-size analysis, lattice constants refinement, Rietveld analysis, ab initio structure determination. PDXL is a one-stop full-function powder diffraction analysis software suite. The modular design, advanced engine and user-friendly GUI have been satisfying both experienced and novice users since PDXL was released in 2007.
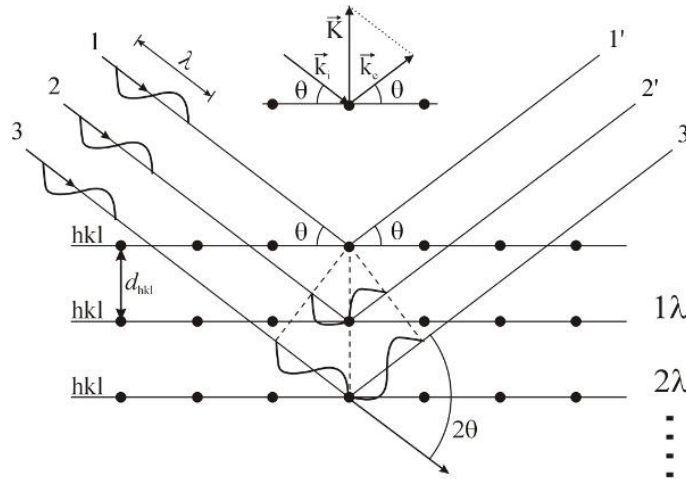

Figure 3: schematic drawing of of the X-ray differation on the sample surface

The data obtained based on Bragg's equation for diffraction which as following:

$$2d \sin \theta = \lambda$$

Where

27

d: Lattice interplanar spacing of crystal (sample)

θ: X-ray incidence angle (Bragg angle)

λ:Wavelength of characteristic X-rays due to the X-ray tube

The lattice interplanar spacing d can be calculated by measuring the Bragg angle θ . By referring the pattern of the lattice interplanar spacing d to standard data such as ICDD (International Center for Diffraction Data) data, it is possible to identify these small crystals. This is the basic principle behind X-ray diffraction.

4.2 Scanning electron microscopy (SEM)

Scanning electron microscopy (SEM) as performed using LYRA 3 Dual Beam (Tescan) equipped energy dispersive X-ray spectrometry (EDX, Oxford Instruments) operated at an acceleration voltage of 30 kV. 2.2.5. BELsorp mini.

The sample holders prepared and cleaned with ethanol to remove all the possible contaminations. A carbon tape was putted on the top of the holder and also cleaned with some ethanol solvent to insure the best cleaning.

Few milligrams of the samples were added to little amount of ethanol and well mixed by shaking to insure good dispersion on the sample powder on the holder. The samples then coated with gold coating with 5 nm thickness using a sputtering coating system to get homogenous coating.

To get the best images a comprehensive set of professional algorithms for image processing and analysis was used to accentuate desirable characteristics of an image, such as brightness & contrast correction, sharpening or noise reduction. Atlas software was used to control the process and provide the best image and it's a combination of a fully compatible offline tool for SEM image manipulation and a powerful image grabber for acquiring static or live images from

optical devices. Atlas represents a complementary stand-alone software solution for your laboratory.

Figure 4: LYRA 3 Dual Beam (Tescan) used for samples analysis

Elemental microanalysis using characteristic X-Rays (EDX) was also provided in this system to analysis the chemical composition information for the SEM images.

4.3 Brunauer–Emmett–Teller theory for porosimeter (BET)

The theory of BET was published first time in 1938 by three famous scientists (Brunauer–Emmett–Teller) in journal of American chemical society. This theory was built based on previous theory of Langmuir for adsorption. Langmuir theory was talking about monolayer type of adsorption but the BET theory extended that for multilayer. The concept of multilayer assumed mainly two assumptions which are the physical adsorption on the solid layers infinitely

and no interaction between each adsorption layer so the Langmuir theory applied on each layer separately. The equation that describes the BET theory is as following:

$$\frac{1}{v\left[(p_0/p) - 1\right]} = \frac{c-1}{v_m c}\left(\frac{p}{p_0}\right) + \frac{1}{v_m c},$$

BEL Japan porosimeter used with liquefied N_2 adsorption at -196°C. the pretreatment done by degassing the sample at 350 ^{o}C for 12 h. The surface area, pore volume and pore size distribution were reported based on the BET calculation method.

The easy-to-use ASAP 2020 software which was used can utilize a Windows interface that includes Wizards and applications to help plan, launch, and control the analysis. All the BET calculations for the surface area, pore volume and pore size distribution are automatically calculated and all the results were presented in a Microsoft excel sheet.
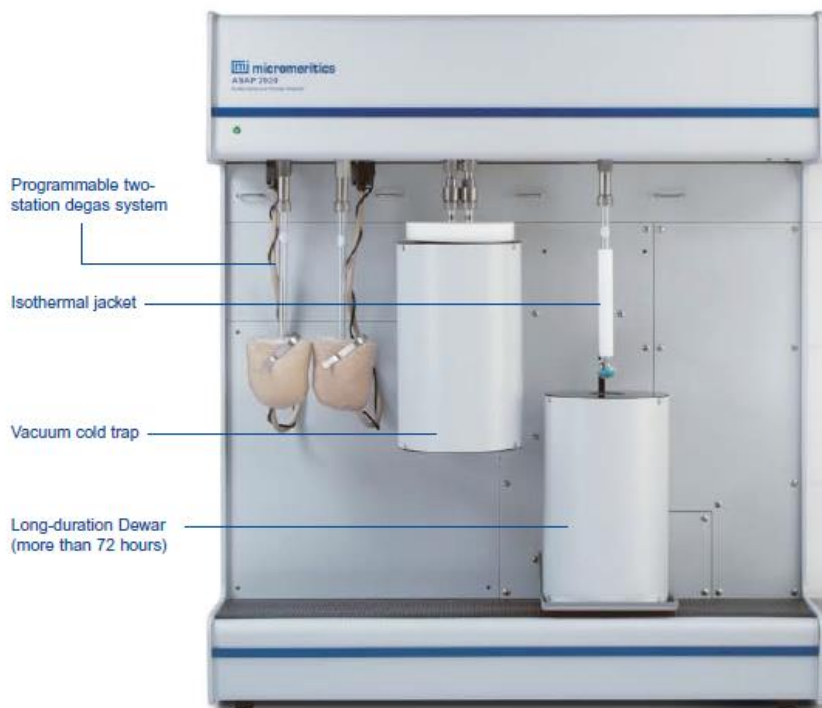
Figure 5: Accelerated Surface Area and Porosimetry System (ASAP 2020)

4.4 Temperature Programmed Desorption (NH$_3$-TPD)

The acidity calculated utilizing ammonia Temperature Programmed Desorption (NH$_3$-TPD) instrument using AutoChem II 2920 which is a fully automated chemisorption analyzer. Unlike the BET which is measuring the physisorption binding energy, the NH$_3$-TPD is utilized to measure the chemisorption interaction which represents the real active sites. These active sites are actually the force that can bind the reaction on the surface of catalyst and offer the suitable condition for reaction to take place. The chemisorption can offer only one layer of molecular to be attached to the surface which is different from the physisorption which can allow multi-layers to be attached.The NH$_3$ was carried out by He with 1% balance. The heating rate was 5 ^{o}C /min and the data were recorded from 200 to 600 ^{o}C.

Figure 6: Automated Catalyst Characterization System (AutoChem II 2920)

CHAPTER 5

RESULTS & DISCUSSIONS

5.1 Synthesis parameters

The presence of as-synthesized Na-EU-1 was confirmed from XRD patterns as shown in Figure 7. An XRD pattern reported by Xu et al. was used as a standard [6]. This figure confirmed the existence of all the major peaks of EU-1 in the synthesized sample.
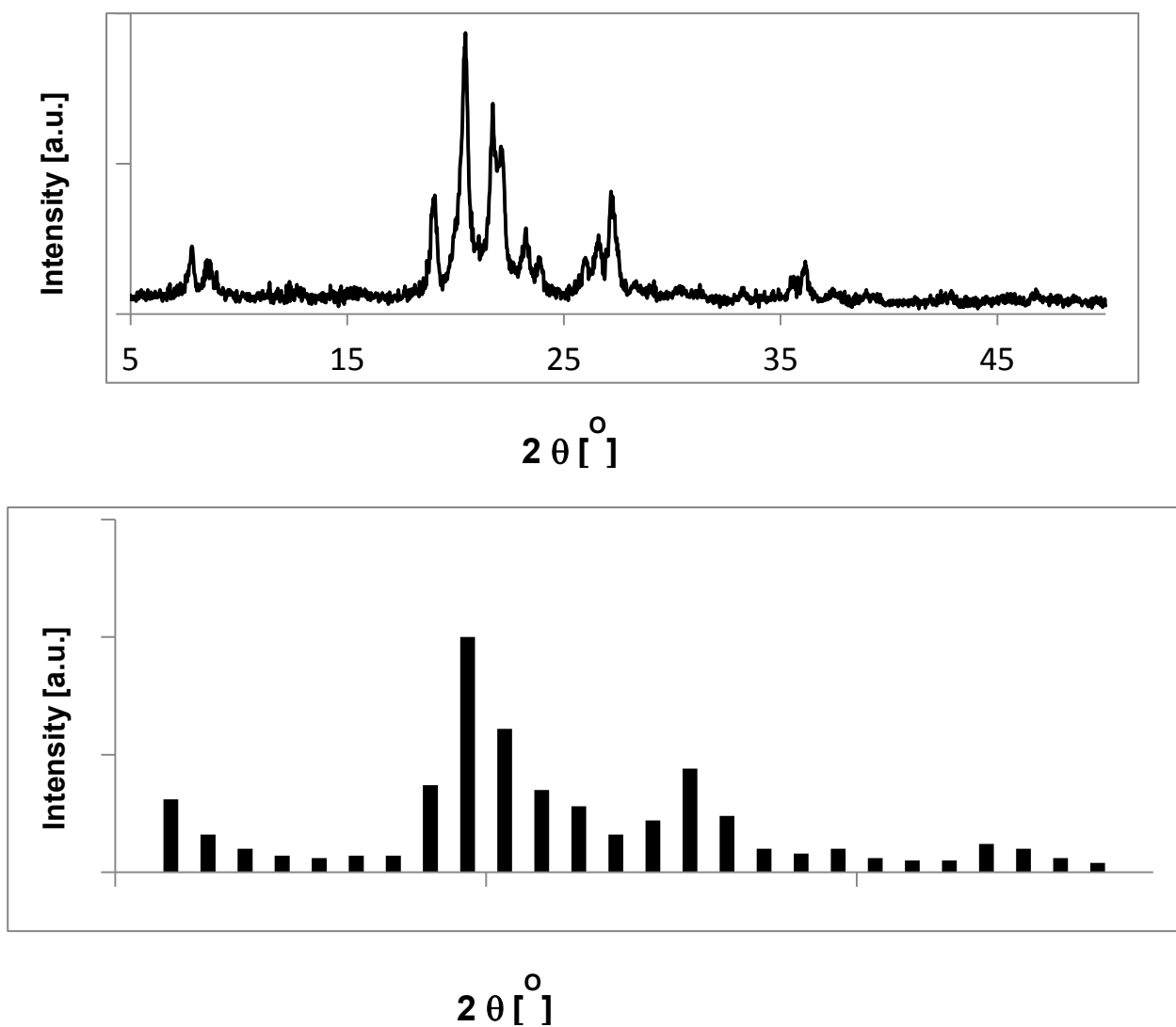

Figure 7: XRD patterns of EU-1 zeolite in comparison with reference [4].

5.1.1 Effect of aging time

Figure 8 shows XRD patterns of Na-EU-1 synthesized with different aging times from 3 to 24 h. The crystallinity of samples was analyzed using XRD software (PDXL). By increasing the aging time, crystal size changes slightly in the nanometer range (see Table 4). Maximum degree of crystallinity was obtained after 12 h of aging time [78, 79]. This EU-1 sample obtained after 12 h aging time was used as a standard for crystallinity calculation. Prolonged aging time contributed positively to crystallinity of EU-1. When the aging time was prolonged from 3 to 12 h, the crystallinity increased. However, when longer aging time (24 h) was applied, some impurities were observed at 2θ of 21.7 which is overlapped on EU-1 peak as shown in Figure 8., this peak has been confirmed as a characteristic peak of cristobalite phase [3] The impurities are shown by SEM micrographs in Figure 9.

Table 4 : Crystallinity and crystal size of EU-1 at different aging times.

Aging time [h]	Crystallinity [%]	Crystal size* [nm]
3	44.6	51.2
6	71.4	49.7
12	100	47.5
24	66.8	30.7

* The crystals size has been determined by XRD

Figure 9 shows the petal-like crystals, which were obtained with different aging times. The morphology is similar with other study on EU-1 as reported elsewhere [6]. The prolonged aging time affected crystal size, agglomeration rate and external morphology of EU-1. For aging time of 3 h, relatively large crystals of ca. 51 nm were observed. The nanocrystals formed large agglomerates of 2 μm and the presence of the amorphous phase was obvious.
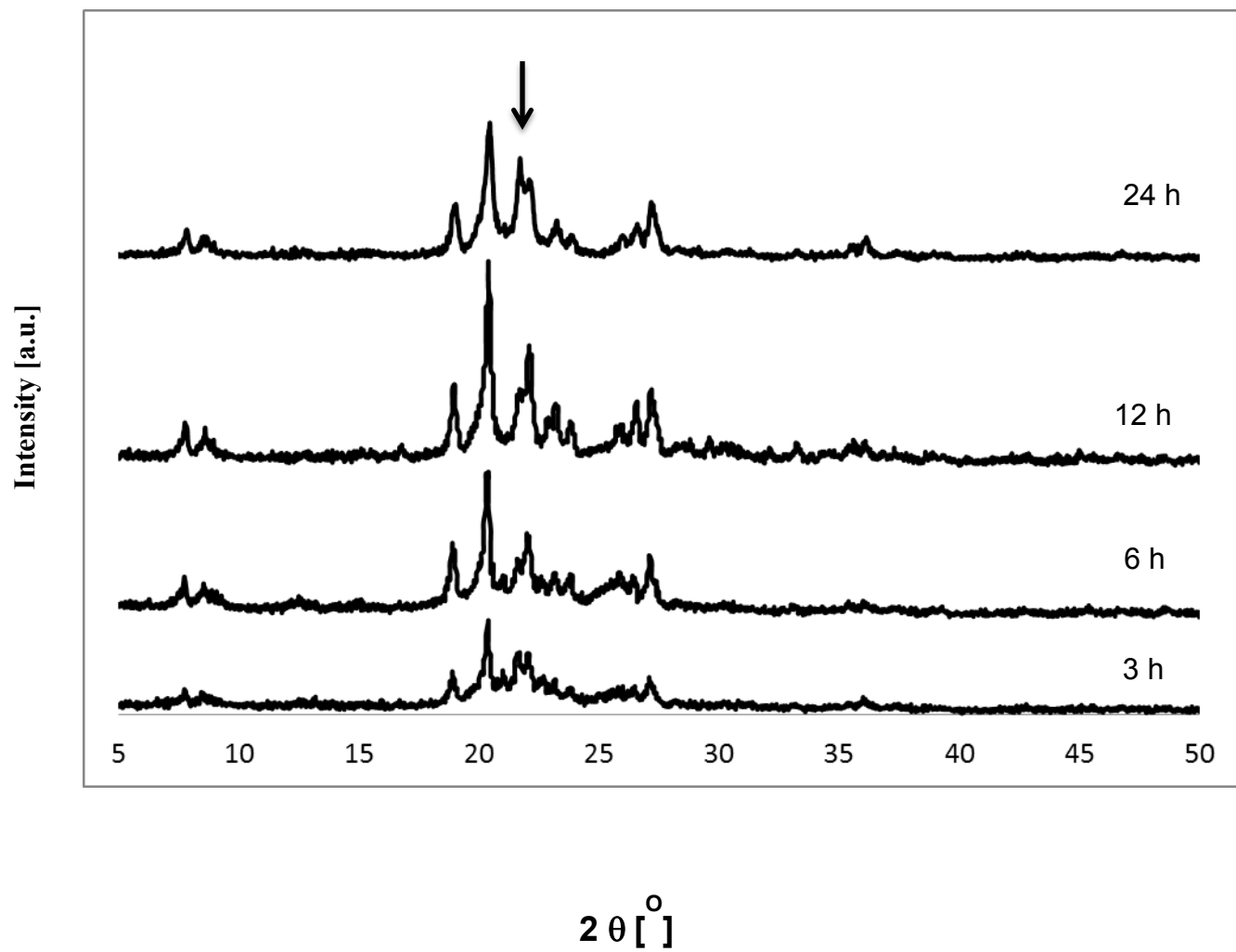
33

Figure 8: XRD patterns of EU-1 synthesized with different aging times.

Increasing the aging time to 6 h reduced the crystal size to 49 nm with smaller portions of non-crystalline phase. Larger agglomerated particles (3-4 μm) were observed. In case of 12 h aging time, smaller nanocrystals of 47 nm were observed with highest crystallinity without amorphous phase. However, the agglomerates became larger (4-5 μm). When we further increased the aging time to 24 h, very small crystals with size of ca. 30 nm were produced. The agglomerated particles were very large (8-10 μm). Unfortunately, a significant amount of dense phases (impurities) was observed clearly. Therefore, the optimum crystal size with full crystallinity was obtained with aging time of 12 h. Smaller crystal size contributes to better mass transfer in catalytic reactions. For other results, an aging time of 12 h was used throughout this paper.

5.1.2 Effect of synthesis temperature

Synthesis of EU-1 zeolite is sensitive to temperature change. We found that changing the synthesis temperature in a narrow range (190 ^{o}C ± 5) affected the zeolite crystallinity as shown by XRD patterns in Figure 10. The maximum crystallinity was achieved for synthesis at 190 ^{o}C for 72 h. Small increased or decreased of the temperature reduced the crystallinity as shown in Table 5. When the crystallization temperature was decreased to 185 ^{o}C, the crystallinity decreased slightly from 100 to 98.1%. The difference in crystallinity is also clear from SEM micrographs in Figure 11. The significant effect of temperature on crystallinity was also reported for other zeolite frameworks, MFI and LTA [80, 81].
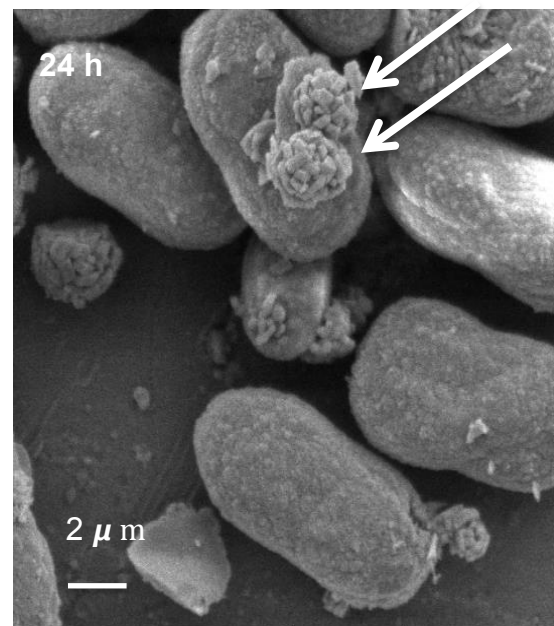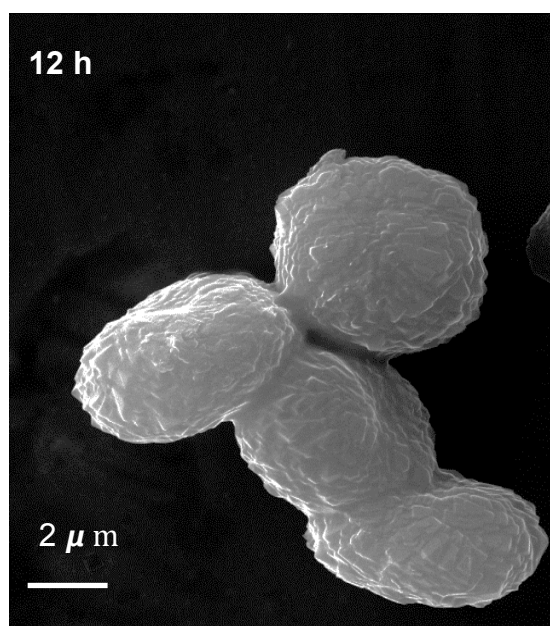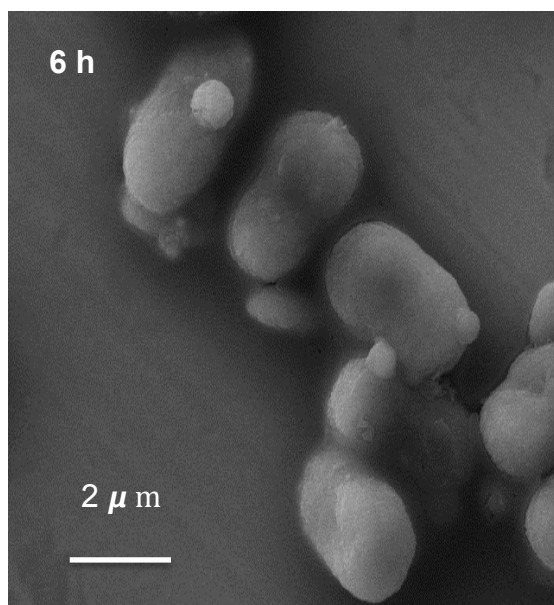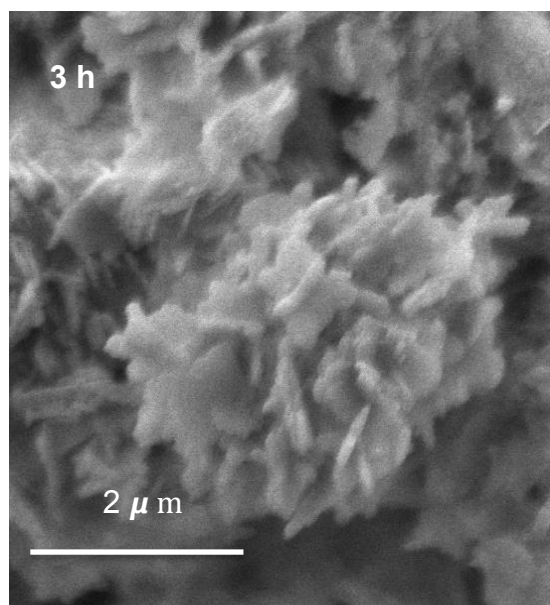
Figure 9: SEM images of EU-1 synthesized with different aging times.

Table 5: Crystallinity of EU-1 at different synthesis temperatures.

Synthesis temperature [^{o}C]	Crystallinity [%]
185	98.1
190	100
195	73.1
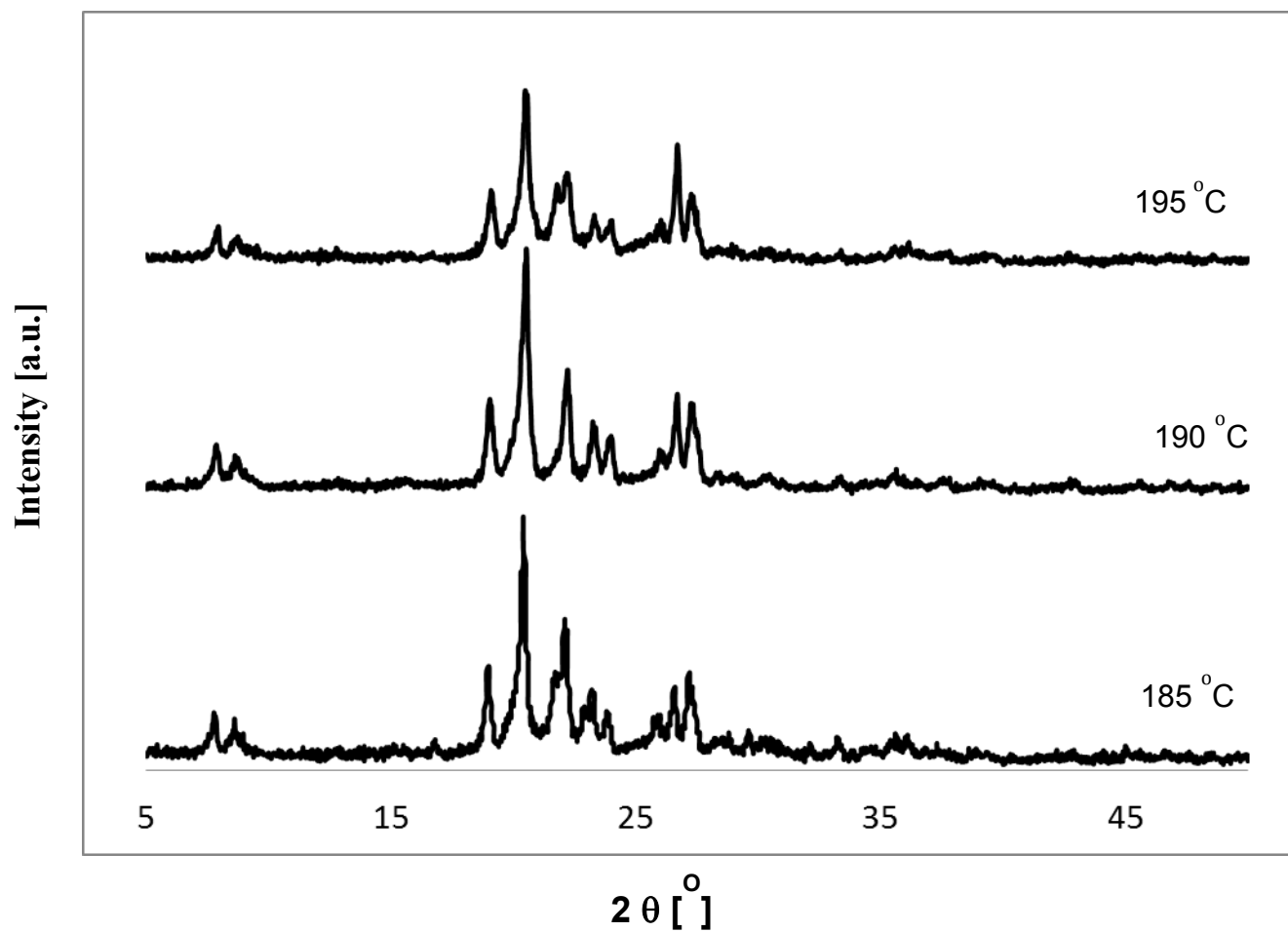
Figure 10: XRD patterns of EU-1 synthesized with different synthesis temperatures.
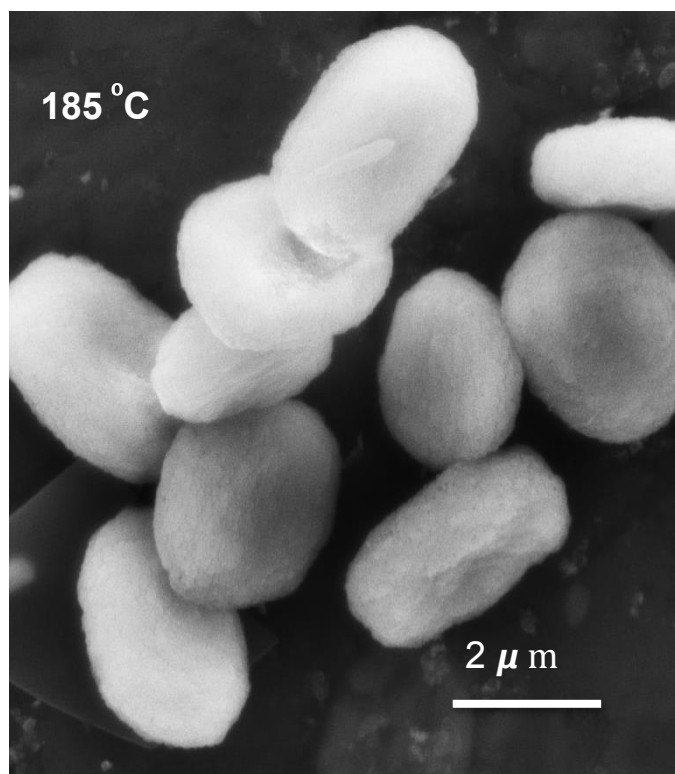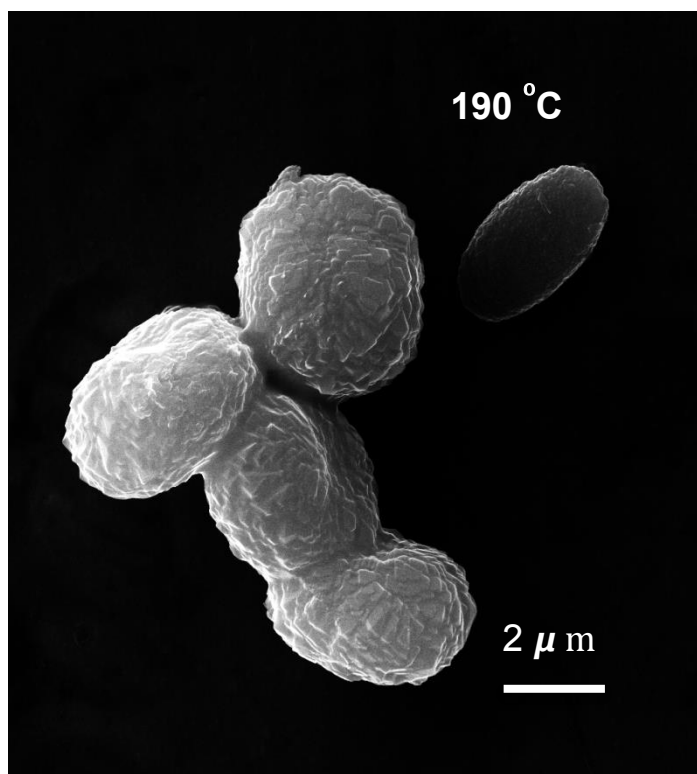
Figure 11: SEM images of the EU-1 synthesized at different synthesis temperatures.

5.1.3 Effect of synthesis time

Figure 12 shows XRD patterns of Na-EU-1 synthesized at different synthesis times from 24 to 72 h. When the synthesis time was 24 h, amorphous phase was obtained. An increase of synthesis time to 48 h, resulted in partially crystalline Na-EU-1. These results show that the minimum time to synthesize crystalline EU-1 zeolite was 72 h. A similar trend was reported for different zeolitic phases, for instance, crystallinity increased with synthesis time for LTA and MFI zeolites [78, 79, 81, 82].
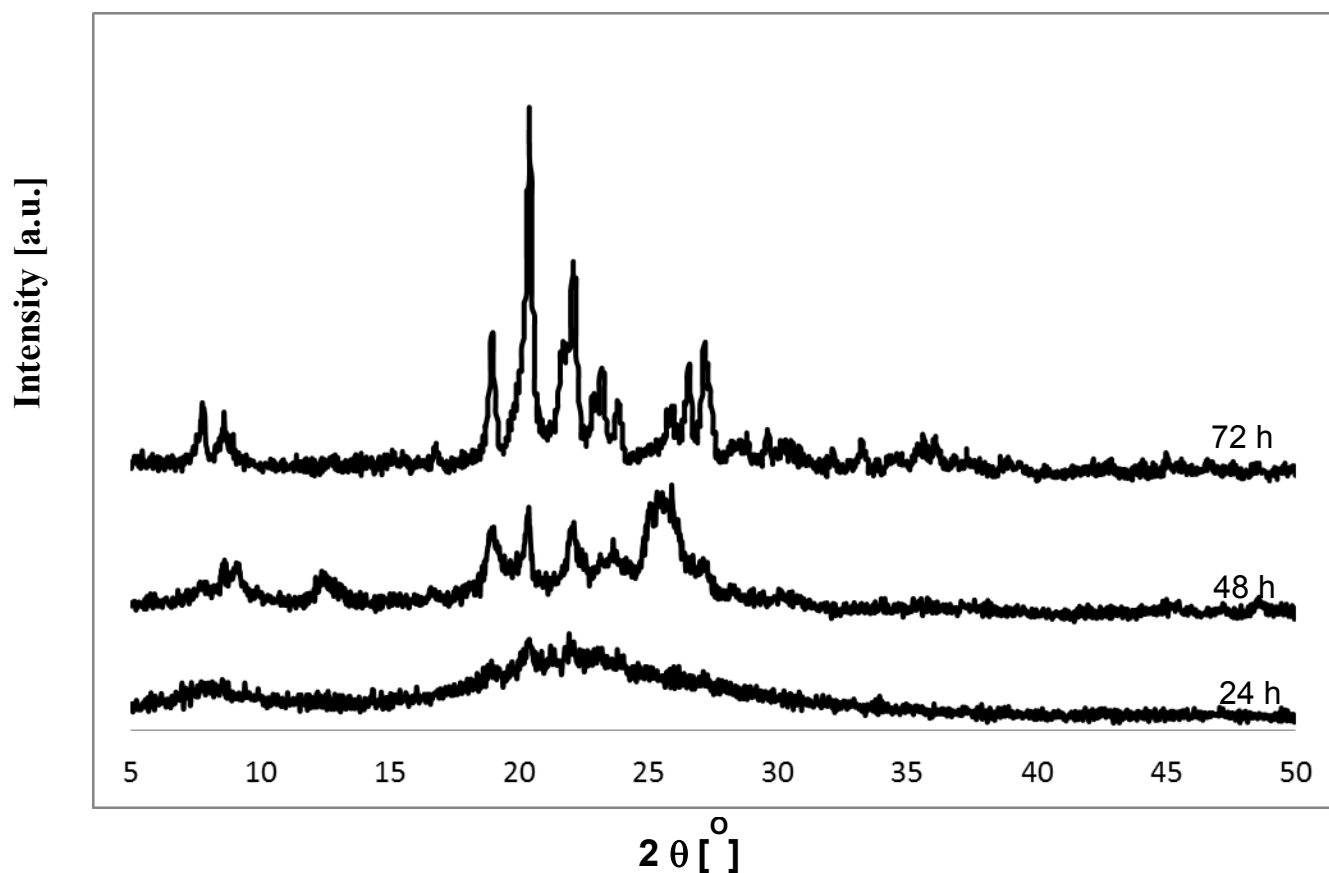
Figure 12: XRD patterns of EU-1 synthesized for different synthesis time.

5.2 Effect of desilication on EU-1 crystallinity

The XRD analysis was used to study the effect of disilication on the crystallinity. It was observed that as the desilication time increased, the crystallinity was initially decreased until reaching a steady-state condition where the solution was saturated with Si species and the extraction of Si became more difficult. At this prolonged desilication, extractions had no more effect for long term treatment, and the dislocation reached a plateau. The three sets of XRD patterns in Figure 13 (a, b and c) describe the implication of desilication on crystallinity.

The effect of NaOH concentration on the zeolite structure was almost similar to the effect of desilication time. Increasing the concentration of basic solution lowered the zeolite crystallinity. However, at high concentration, for instance, when 1 M of NaOH was applied for 60 min, severe extraction of Si species also impacted the removal of Al species from the frameworks as the Si-O-Al chains are interconnected. The XRD pattern of a sample treated with 1 M of NaOH for 60 min confirms that the zeolite crystal structure starts to change and collapse by the severe condition (harsh) Si removal. Instead of creating mesopores on the zeolite surface, large pores were created. In some cases at severe condition, the pores can reach hundreds of nanometers.

The XRD patterns are also very helpful to observe the effect of NaOH concentration as shown in Figure 14.

The crystallinity of modified EU-1 is presented in Table 6. The crystallinity percentage was calculated according to the strongest XRD peaks for parent sample.

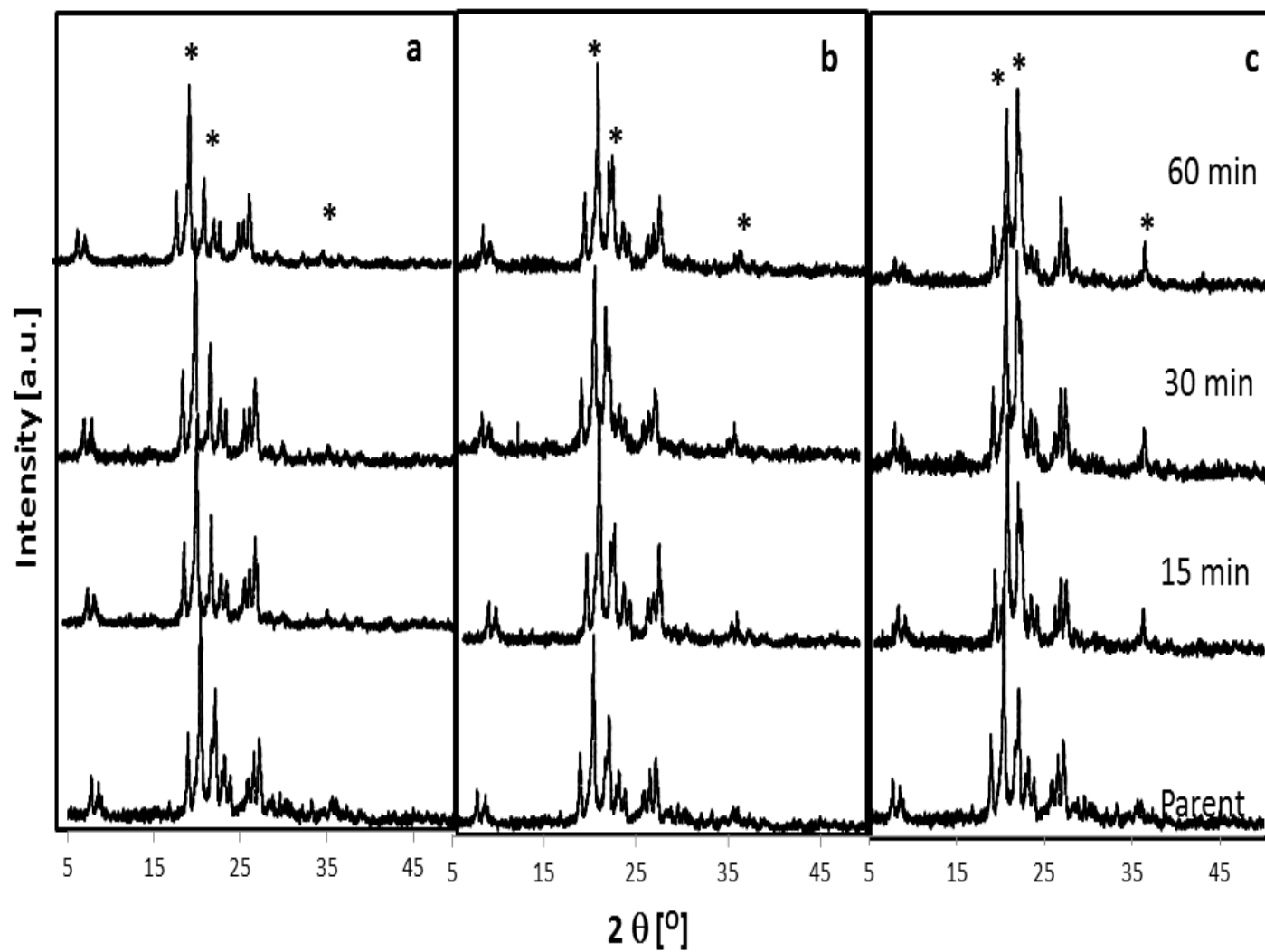**Figure 13: XRD patterns of parent and desilicated EU-1 samples at different NaOH concentrations: a. 0.25 M.   b. 0.5 M.   c. 1 M**
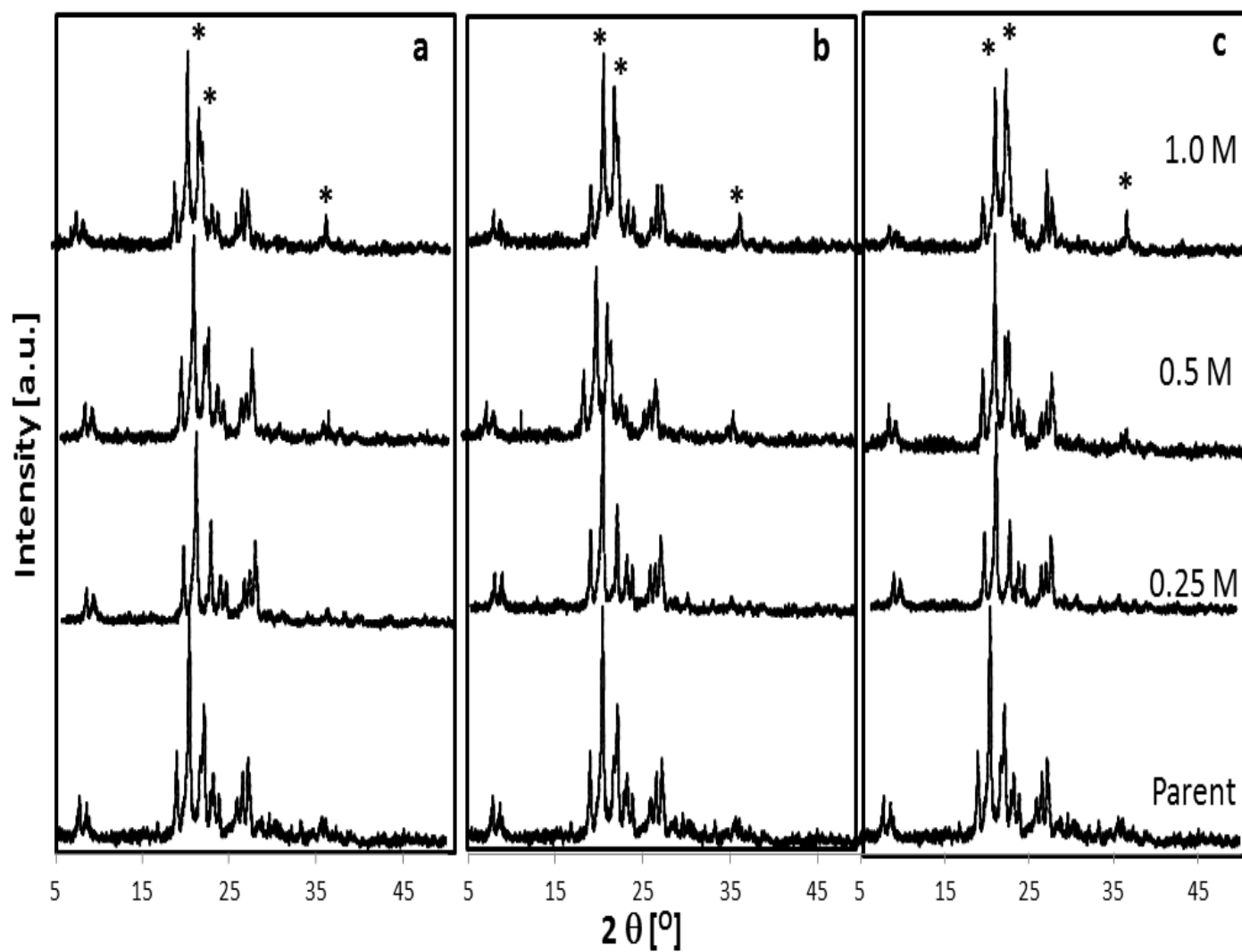
Figure 14: XRD patterns of parent and desilicated EU-1 samples at different times: a. 15 min. b. 30 min c. 60 min.

Table 6: Crystallinity of desilicated samples as a percentage of parent.

Concentration Time (min)	Crystallinity (%)		
	0.25 M	0.5 M	1 M
15	88.3	81.1	61.9
30	85.9	66.7	61.2
60	82.9	57.8	55.9

5.3 Effect of desilication on EU-1 morphology

The introduction of the mesopores on the external surface of EU-1 zeolite was elaborated with SEM and TEM analysis. The presence of defects created by alkaline treatment is shown by arrows in Figure 15. The TEM micrographs in Figure 16 also confirmed the appearance of mesopores on the surface in the range from 10 to 20 nm, especially for the sample treated with 0.5 M of NaOH. Figure 16 shows different TEM micrographs for EU-1 samples treated for 60 min with different NaOH concentrations from 0.25 to 1 M. The presence of mesopores is clearly presented by TEM micrographs. The formation of mesoporosity was very clear when 0.5 M of NaOH was used for 60 min in desilication. However, more severe condition by increasing the NaOH concentration to 1 M was destructive to the structure and the yield of EU-1. The TEM image in Figure 16(d) showed the presences of macroporous (> 50 nm) especially near the edges. In line with TEM studies, SEM micrograph (Figure 17) also shows that macropores formed in desilication of EU-1 zeolites at NaOH concentration higher than 0.5 M. These findings collected from XRD, SEM and TEM results are summarized in the following cartoon (Figure 18).
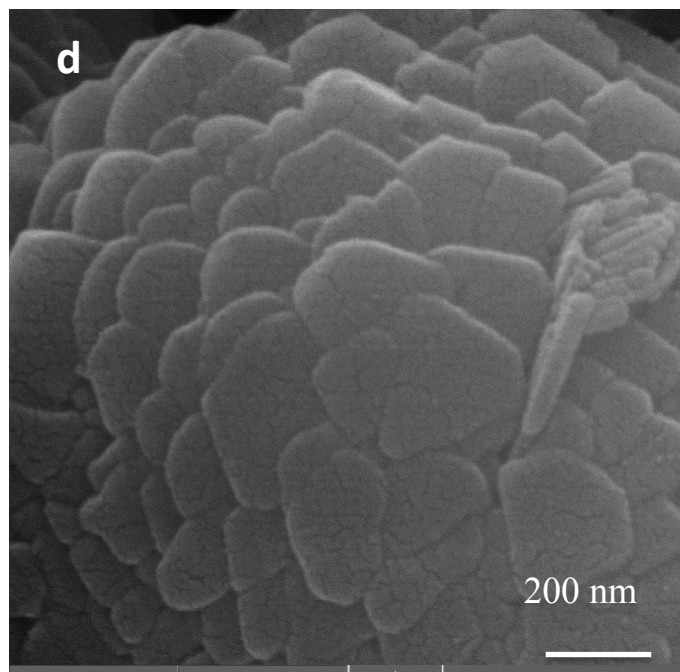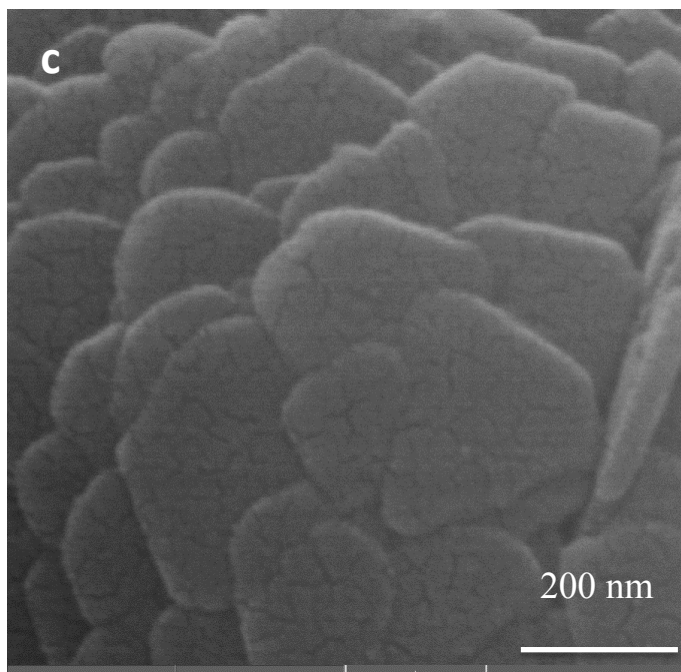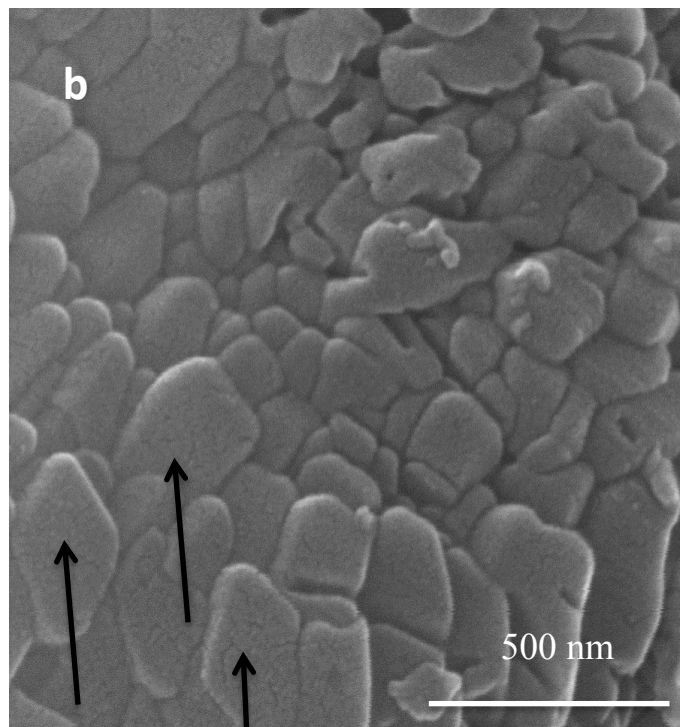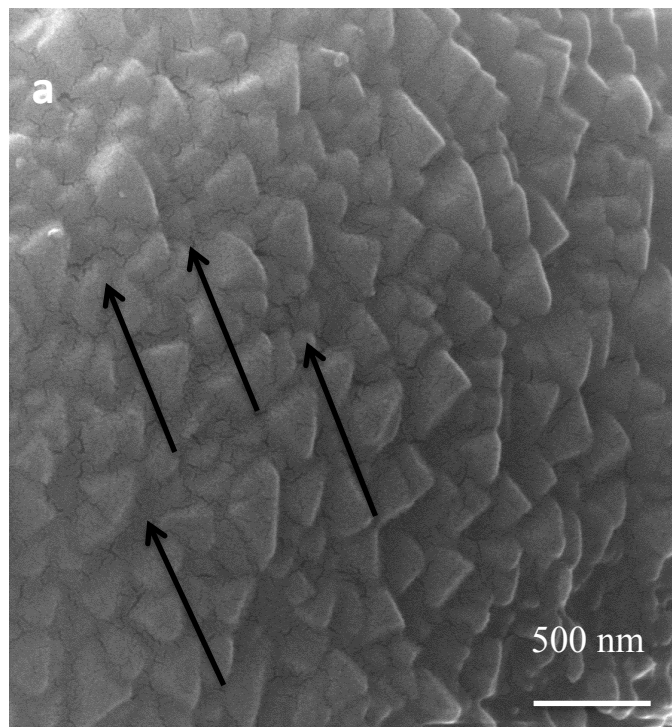
Figure 15: SEM images for treated sample with 0.5 M NaOH , (a) and (b) treated for 30 min (c) and (d) treated for 60 min.
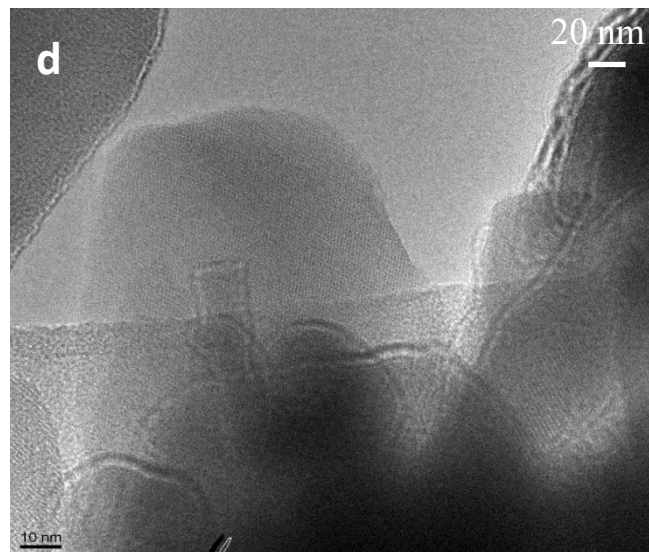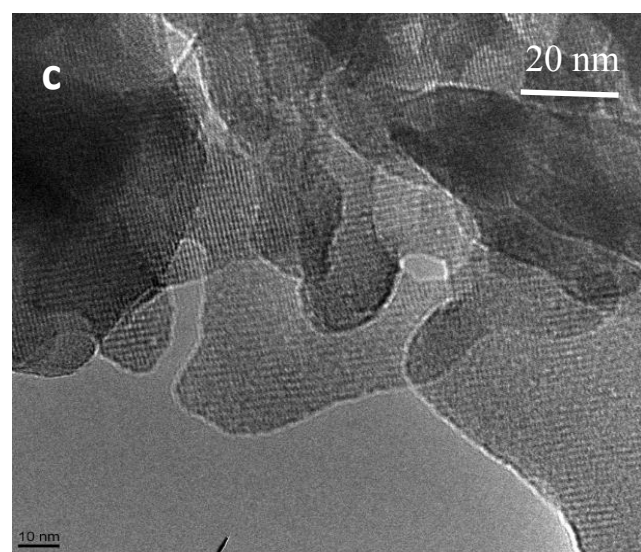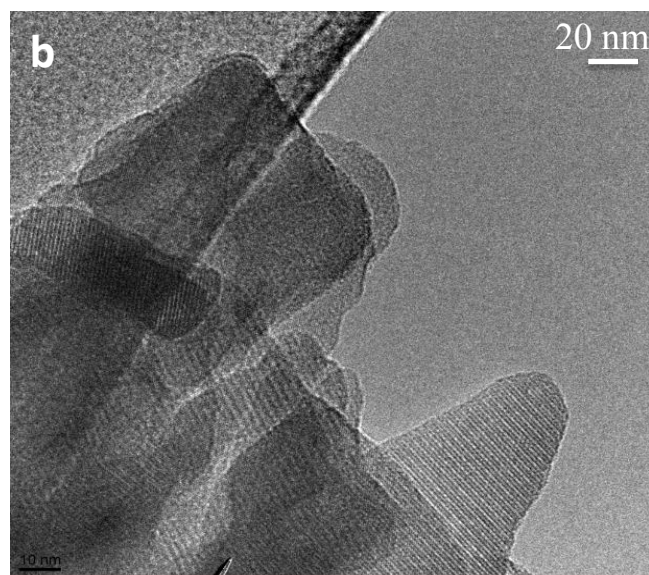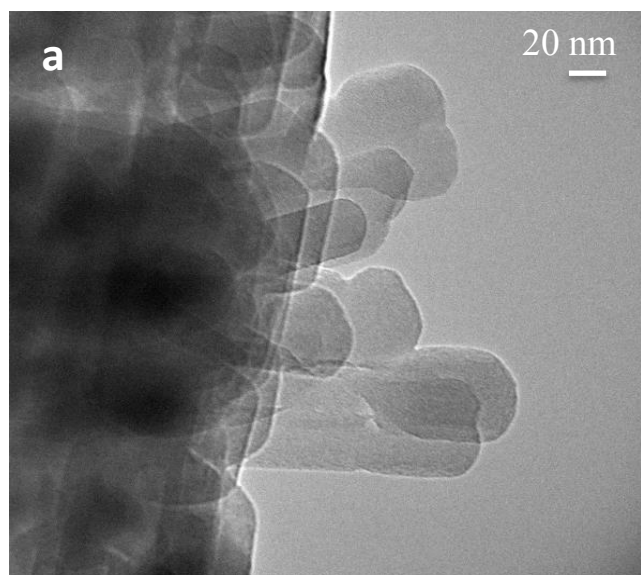
Figure 16: TEM images for parent and disilicated samples treated for 60 min,

(a) Parent, (b) 0.25 M, (c) 0.5 M, (d) 1 M .
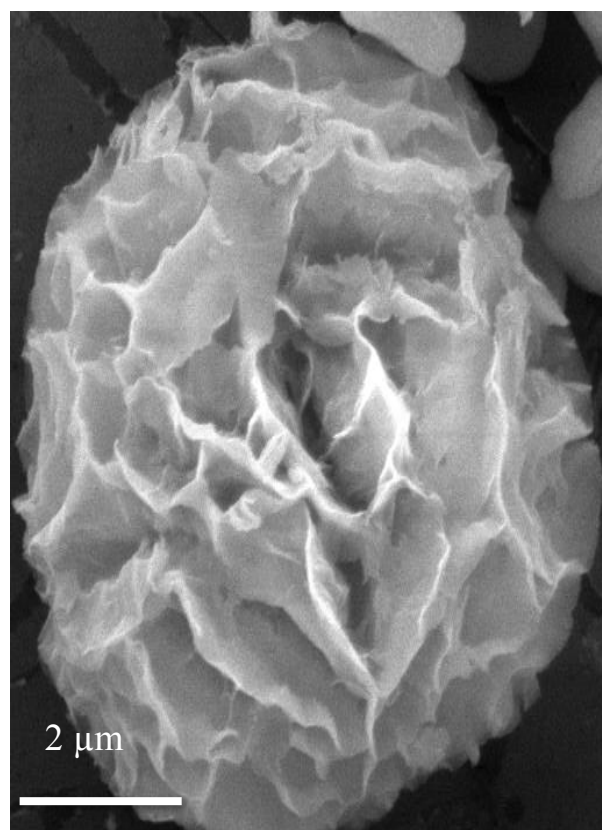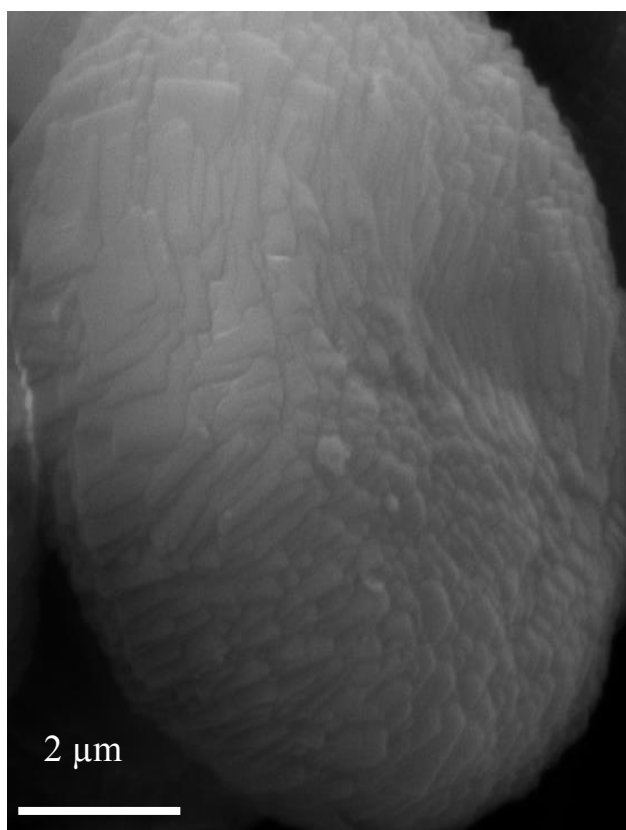
Figure 17: SEM images for parent and harsh desilicated samples with 1 M NaOH for 60 min

5.4 Effect of desilication on Si/Al ratio

The EDX results were used to recognize the composition of elements in the parent and the desilicated samples. The Si extraction depended on the framework structure and how the Al species are located in the framework. In order to investigate the effect of NaOH concentration and treatment time, we analyzed nine treated samples together with the parent and the results confirmed our previous hypothesis on the lowest Si/Al ratio. Minimum Si/Al ratio was achieved with Si/Al of 14.07 after desilication in 0.5 M NaOH concentration for 60 min. Further increases in NaOH concentration to 1 M have a negative effect on the structure of EU-1. Dissolution of both Si and Al species from the framework was observed. With more severe condition (1M of NaOH for 60 min), the Si/Al ratio was increased again. The EDX results from Table 7 also showed that the severity of desilication time has a similar effect on the Si/Al ratio as previously found for desilication time's effect on crystallinity. The cartoon in Figure 18 elucidates the idea of how the Si/Al ratio started to increase again with the increasing of NaOH concentration to 1 M.

Table 7: EDX results of desilicated samples (Si/Al).

Concentration Time (min)	Si/Al		
	0.25 (M)	0.5 (M)	1 (M)
15	17.4	17.34	16.8
30	17.1	17.12	16.6
60	16.7	14.07	16.5

NaOH

0.25

NaOH

0. 5 M

NaOH

1 M

Deposited
Al- species
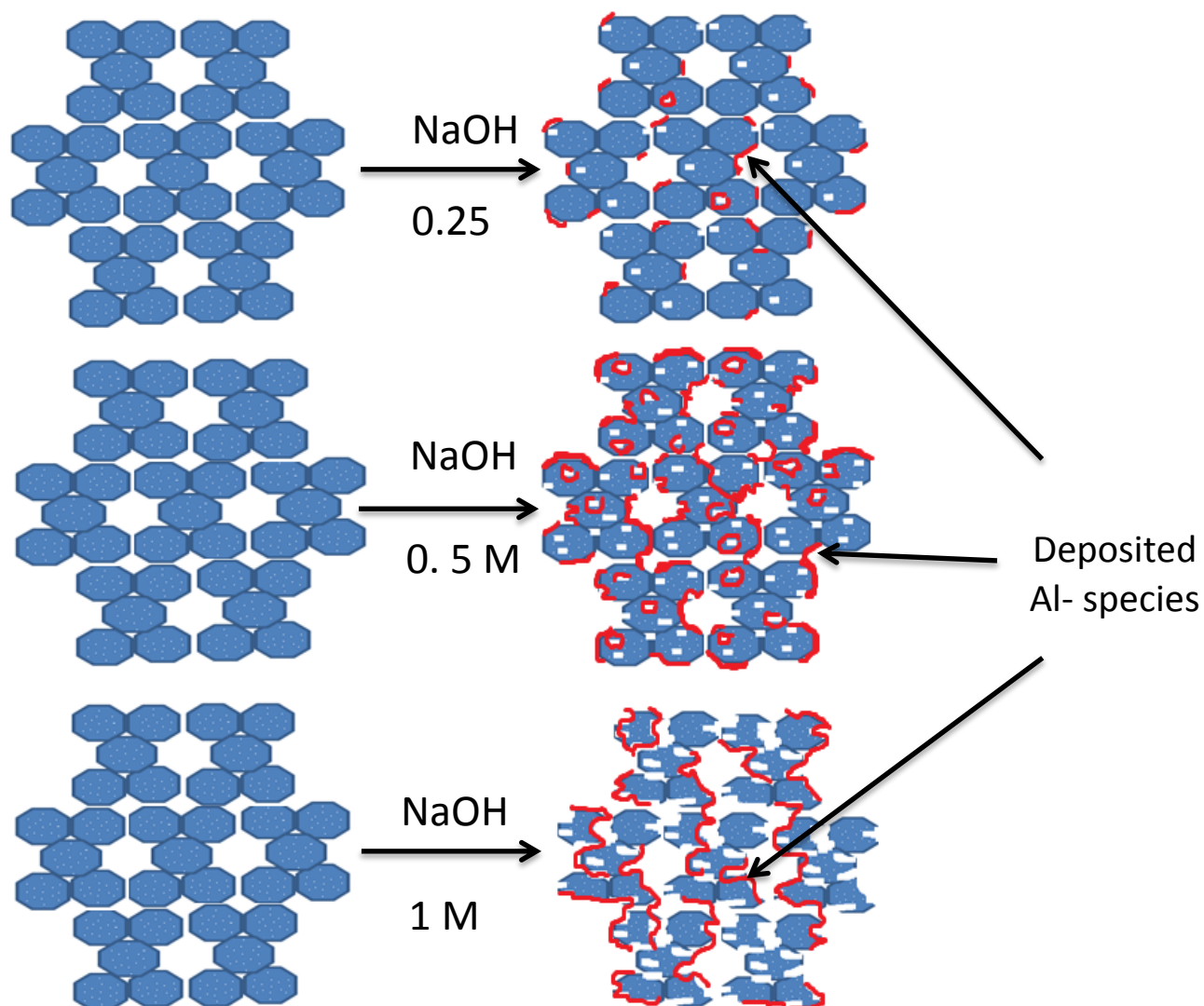
Figure 18: Effect of NaOH concentration on the EU-1 zeolite structure.

5.5 Effect of desilication on the textural properties of EU-1

The alkaline post-treatment with 0.25 M at 80°C for 60 min has a positive influence on the mesopore volume of EU-1. The mesopore volume was slightly increased to 0.081 cm^3/g. This pore volume is the best mesopore volume within this work. The microporosity decreased from 0.088 to 0.079 cm^3/g (Table 8). Further increases in NaOH concentration to 0.5 and 1 M yielded a negative impact on both meso- and microporosity. Verboekend et al reported in the case of ZSM-22, another one-dimensional pore zeolite, the surface area and pore volume after desilication was reduced due to the presence of dissolved non-framework Al species, which deposited on the external surface of the crystals and inside the pores [70]. In addition to Al dissolution, severe treatment with 1M of NaOH extensively extracted Si and Al species, which led to the formation of macroporosity (pores> 50 nm). The micropore volume of hierarchical EU-1 indicated reverse proportional relation with the NaOH concentration, the higher the concentration of NaOH, the lower the micropore volume. The lowest micropore volume observed with 1 M of NaOH (0.038 cm^3/g). The corresponding nitrogen adsorption desorption isotherms are presented in Figure 19.

The above discussion on the effect of alkaline concentration has been confirmed by the BJH-pore size distribution as shown in Figure 20. Parent EU-1 samples contain mainly microporosity (< 2 nm) with the minor existence of mesopores.

After the mildest treatment with 0.25 M of NaOH, the distribution of pore size was shifted from small mesoporosity zone (10-30 nm) to the large mesoporosity zone (30-50 nm) with decreasing amount of micropores. When the samples were treated with higher NaOH concentrations, the appearance of macropores (> 50 nm) was observed clearly and large decrease in the both micro-

and mesopores are being reported. Generally, we may conclude here that the alkaline concentration was the most crucial parameter for the distribution of the pore size in hierarchical zeolites.

The decreasing tendency of BET surface area results of EUO (EU-1) zeolite when the NaOH concentration was increased were reported elsewhere for another one dimensional pore zeolite, ZSM-22 [70]. The small pore size of both EUO and TON zeolites affects difficult extraction of Si species from the framework as compared with three-dimensional pore zeolites (for instance ZSM-5 (MFI). Strangely, the mesoporosity of the sample treated with 0.25 M of NaOH was not increased. In fact, the mesopore surface area was even dropped to 43 m^2/g.

Similarly, for other samples treated with higher concentration of sodium hydroxide, the S_{micro} and S_{meso} area were both decreased. With the increase in NaOH concentration, more Al species will deposit on the external surface of EU-1. Therefore, the surface area of micropores was reduced not only by the conversion of micropores to mesopores (and macropores) but also due to the partial blocking by Al deposit.

Table 8: Textural properties of parent and desilicated EU-1 samples.

Sample	S_{total} (m^2/g)	S_{micro} (m^2/g)	S_{meso} (m^2/g)	V_{micro} (cm^3/g)	V_{meso} (cm^3/g)	NH_3-TPD (mmol/g)
Parent	277.0	225.5	51.5	0.088	0.078	0.273
0.25 M	246.1	202.8	43.4	0.079	0.081	0.259
0.5 M	139.4	113.9	24.5	0.044	0.048	0.218
1 M	117.9	97.5	20.4	0.038	0.044	0.143
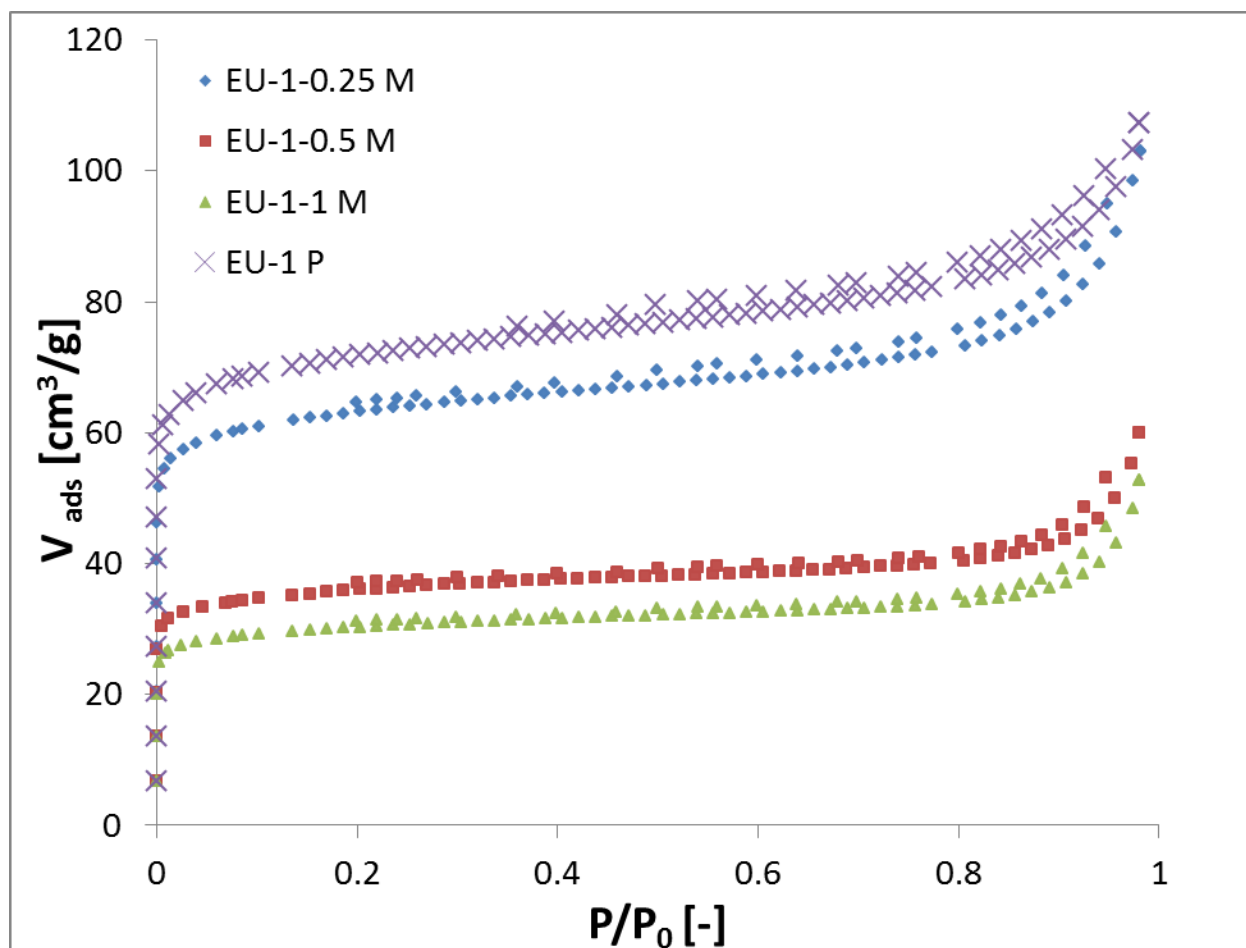
Figure 19: Isotherms plot for N$_2$ adsorption and desorption of parent and desilicated samples for 60 min.
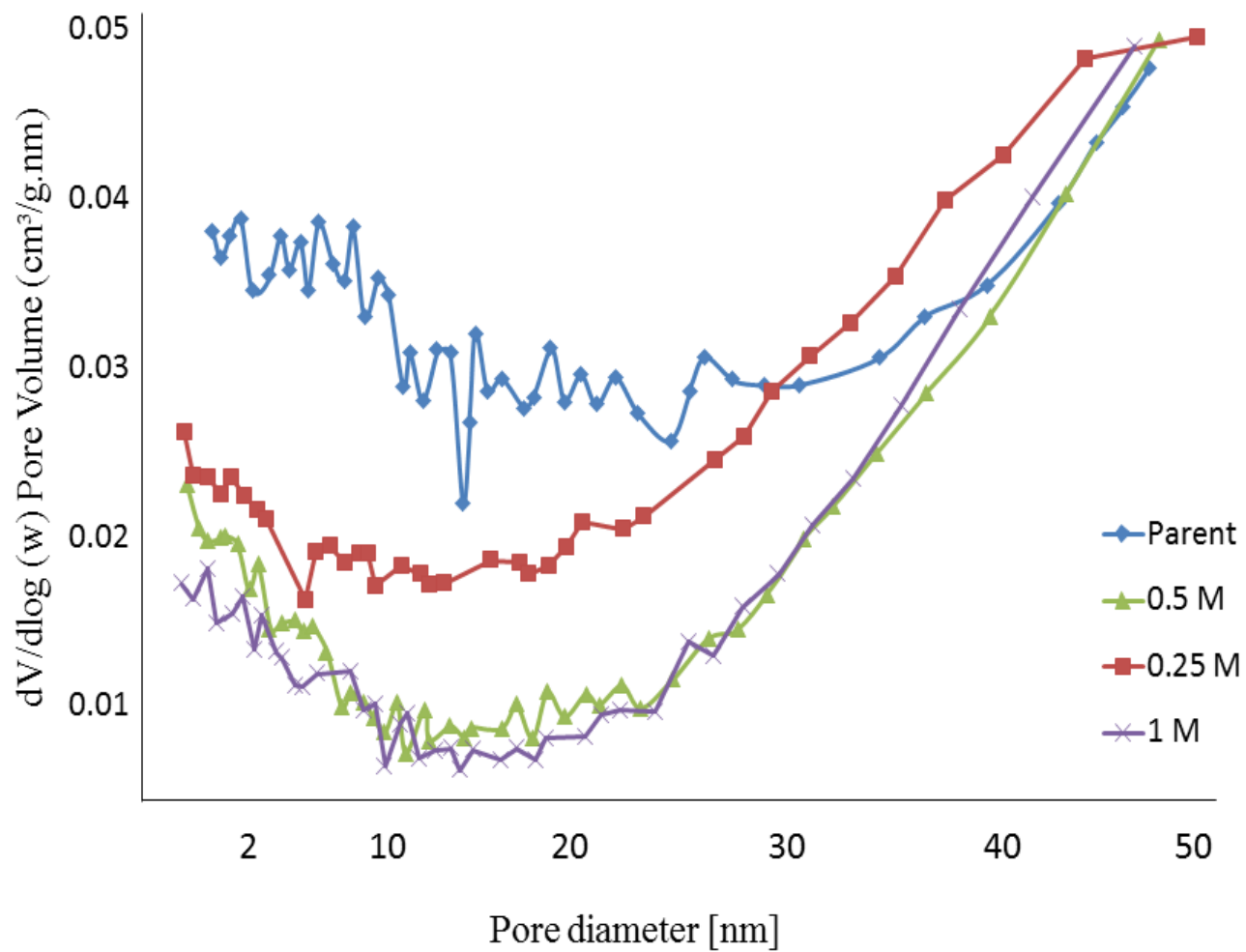
Figure 20: BJH mesopore size distribution of parent and desilicated EU-1 samples for 60 min.

5.6 The effect of desilication on zeolite acidity

As clearly shown in Figure 21, there are two main desorption peaks of the EU-1 parent sample. The strongest peak appeared at 252 ^{o}C, which represents the weak acid site and the shoulder peak is observable around 425 ^{o}C, which represents strong acid site. The NH$_3$-TPD calculation in Table 9 shows good agreement with textural properties derived from BET specific surface area. There was a significant decrease in the amount of desorbed ammonia over EU-1, when the samples were treated with a more severe condition. Especially, for sample treated with 1 M of NaOH, the amount of desorbed ammonia was reduced to approximately a half of the amount in the parent EU-1 sample. With milder alkaline treatment (0.25 M of NaOH), the acidity was just a little being decreased.

5.7 The application of hierarchical EU-1 on dimethyl ether-to-olefins

The parent and the hierarchical EU-1 were applied to the conversion of dimethyl ether (DME) to olefins (DTO). The parent EU-1 sample has the highest conversion of DME (37%) as compared with desilicated samples. This result is acceptable as the dislocation affected both micropore and mesopore volume, which were partially blocked with Al deposit. Furthermore, as reported elsewhere [49], the DME reaction is favored by the weak acidity as the Brønsted acid sites have the ability to bind the methoxy species. The acidity tests from ammonia-TPD confirmed that the parent sample has the highest acidity and desilication reduced the concentration of the acid sites of EU-1.

On the other hand, good improvement was achieved for selectivity toward propylene over ethylene (P/E). The ratio of (P/E) was 1.9 for the parent sample and this ratio jumped to 3.3 for sample treated with 0.25 M. The best justification for this high selectivity toward propylene is

the distinctive structure of treated samples which contain the microporosity and the mesoporosity. The selectivity to propylene over the sample of larger portion of macroporosity (treated with 0.5 M of NaOH) was lower (P/E=2.4). This lower selectivity is caused by the presence of large porosity which is known as macroporosity, which allows higher production of aromatics and large olefins (C5 and C6). Finally, when the sample treated with 1 M, there was no any produced propylene. In addition, very high selectivity toward large compounds such as aromatics, C5 and C6 were observed (almost 86%) as shown in Figure 22.

Concerning the stability of EU-1 catalysts, the parent and the desilicated samples show high deactivation rate. The parent sample lost half of its activity after one hour on stream. The desilicated samples show high deactivation due to the lower surface area as compared with the parent crystals as presented in Figure 22.
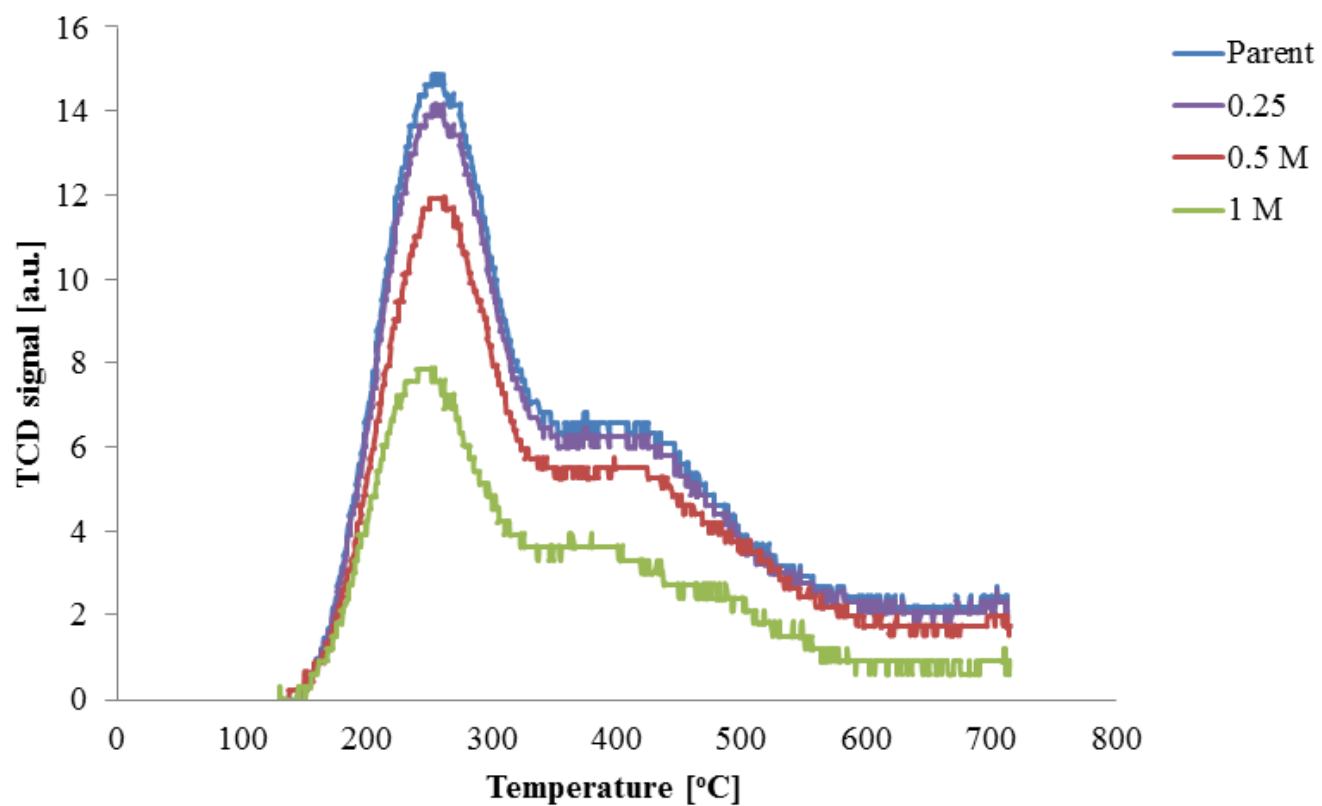
Figure 21: NH3-TPD profiles of EU-1 desilicated samples for 60 min.

5 min after
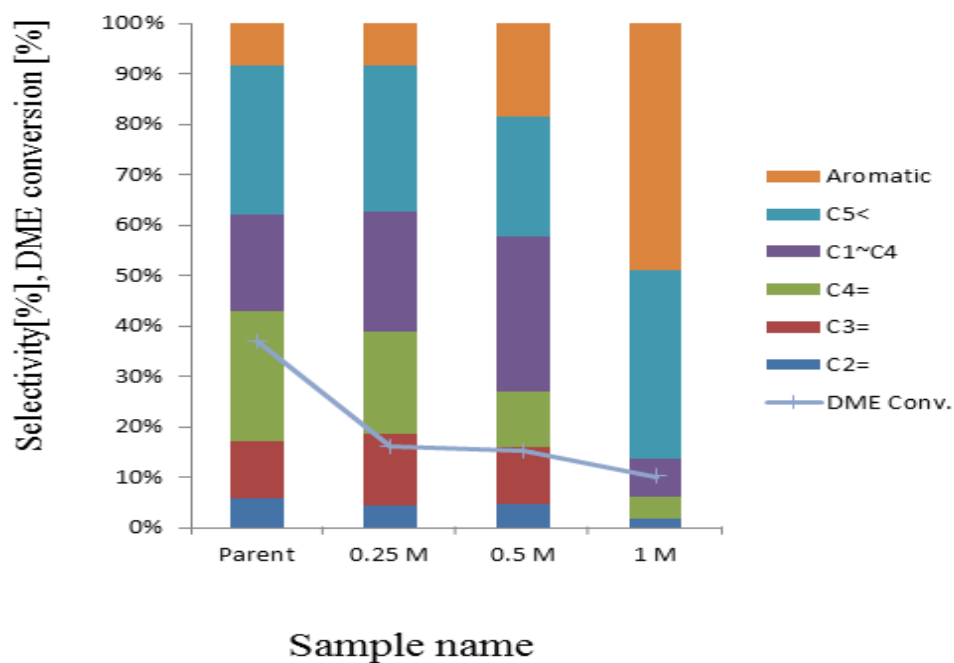
1 h after
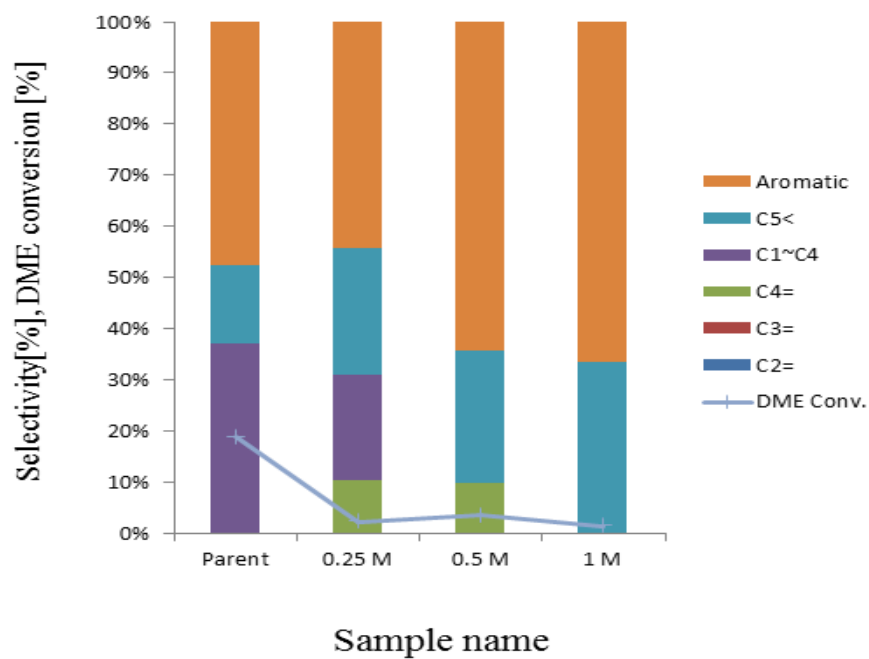
Figure 22: DME to olefins reaction results for parent and desilicated samples for 60 min.

5.8 Calculations of effective diffusivity for desilicated samples
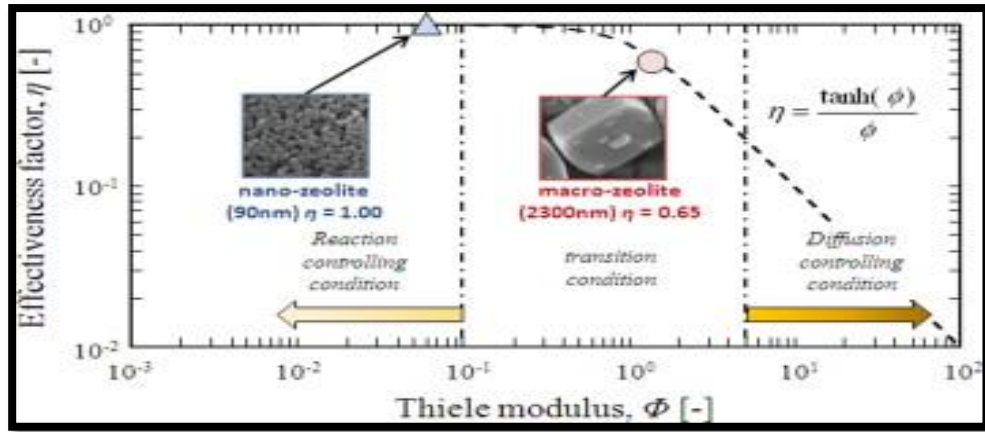
Figure 23 : Relation between effectiveness factor and Thiele modulus [83]

$$\Phi = L \sqrt{\frac{k}{D_{eff}}} \quad [84]$$

$$\eta \, \alpha \, \frac{1}{\Phi} \qquad \rightarrow \qquad \eta \, \alpha \, \frac{1}{L} \qquad \rightarrow \qquad \eta \, \alpha \, D_{eff}$$

- $\eta \, \alpha \, \frac{1}{L} \rightarrow$ Nanosized zeolites
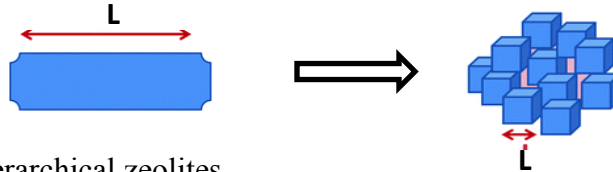
- $\eta \, \alpha \, D_{eff} \rightarrow$ Hierarchical zeolites
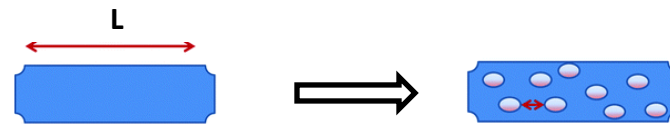
$$D_{eff} = \frac{D_{AB}\emptyset_P \sigma_c}{\tau} \quad [84]$$

Where

$$\emptyset_P = Pellet\ porosity = \frac{Volume\ of\ void\ space}{Total\ volume\ (Voids\ and\ solids)}$$

$$\sigma_c = constriction\ factor$$

$$\tau = Tortusity = \frac{Actual\ distance\ a\ molecule\ travels\ between\ two\ points}{Shortest\ distance\ between\ those\ two\ points}$$

Assumptions:

- As EU-1 has straight channels so $\tau = 1$.

- As there is no variation in the cross-sectional area in EU-1 channels $\sigma_c = 1$.

There for:

$$D_{eff} = D_{AB}\emptyset_P$$

$$D_{AB} = D_o e^{(-\frac{E}{RT})}$$

Given

D_{AB} (T=298) = 1.2 *10^{-9} cm^2/s $\qquad\qquad\qquad$ D_{AB} (T=313) = 1.5 *10^{-9} cm^2/s [85]

After calculations

D_o = 3.95 *10^{-8} cm^2/s $\qquad\qquad\qquad\qquad\qquad$ E= 8.51*10^3 kJ/mol

D_{AB} (T=623) = 7.6 *10^{-9} cm^2/s

Zeolite density= 1.06 g/cm^3

For the base of 1 g of EU-1 zeolite $\qquad\qquad\qquad$ V= 0.943 cm^3

Sample name	Total pore volume (Cm^3/g)	Pellet porosity (-)	D_{eff} at T=298K (cm^2/s)	D_{eff} at T=623K (cm^2/s)
Parent	0.166	0.176	2.1*10^{-10}	1.7*10^{-9}
EU-1 (0.25)	0.160	0.169	2.0*10^{-10}	1.3*10^{-9}
EU-1 (0.5)	0.092	0.098	1.1*10^{-10}	0.74*10^{-9}
EU-1 (1)	0.082	0.087	1.0*10^{-10}	0.66*10^{-9}

5.9 Effect of sequential treatment on EU-1 crystallinity

The XRD results as shown in Figure 24 and Figure 25 elucidate that preserving of characteristic EU-1 phase after the sequential alkaline and acid treatment. Consisting with our previous finding, the effect of increasing NaOH concentration will always decrease the crystallinity either if it followed by acid treatment or not as presented in XRD patterns in Figure 24. These results become reasonable because of existence of amorphous phase of Si and Al species on the surface of the particles together with defects of the crystals structure due to vacant sites after the demetalaion. Unlike desilication the dealumination treatment with HNO_3 was not much destructive for the zeolite crystals as reported for ferrierite, mordenite, TON and BEA zeolites [70, 86-88]. The interesting observation was the increasing of the desilicated samples crystallinity when treated with different acid treatment and this can be explained by removing the deposited non-crystalline phase of Al species on the surface, but also there was slightly decreasing in the crystallinity with the increasing of acid concentrations as shown in Figure 25. The crystallinity calculations presented in Table 9.
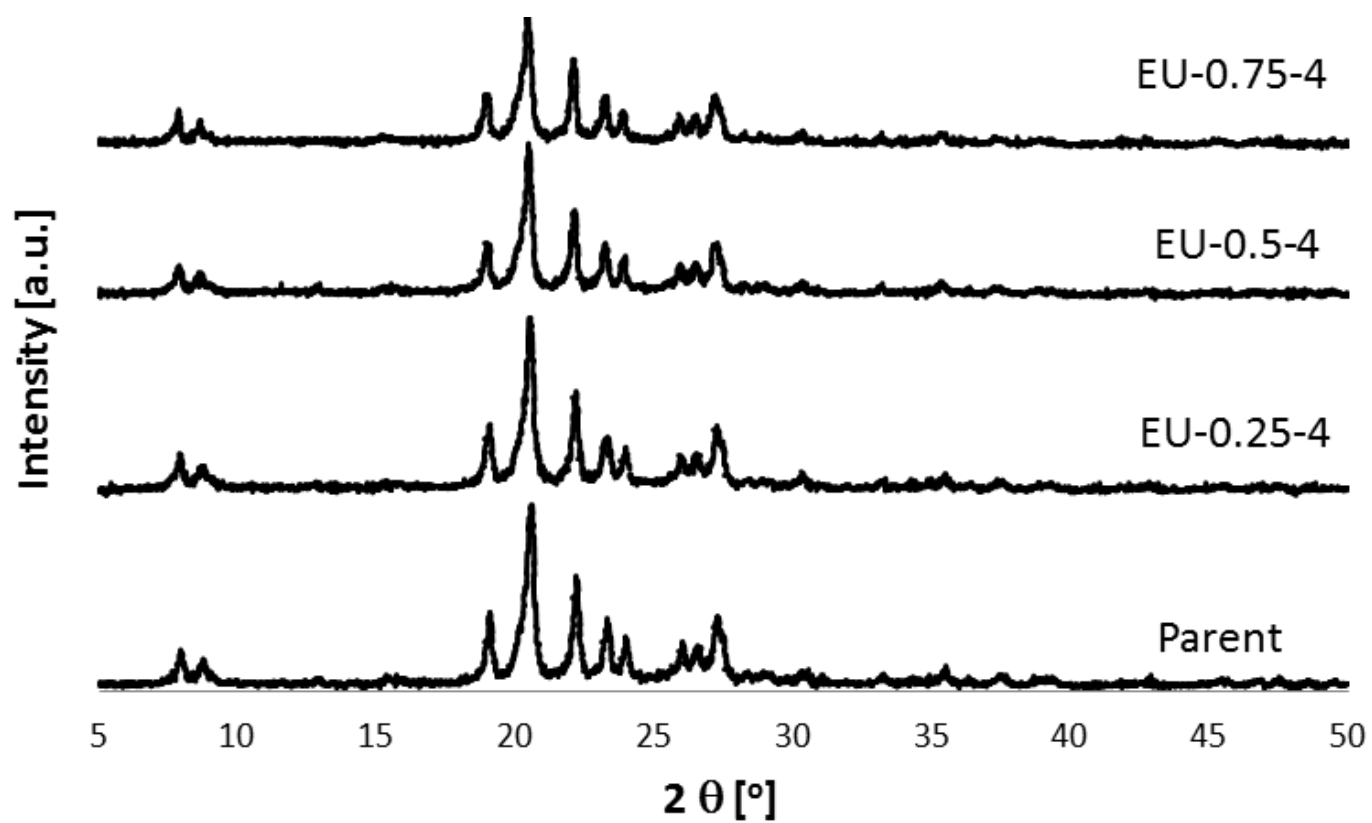
Figure 24: XRD patterns of parent and treated EU-1 samples at different NaOH concentrations.
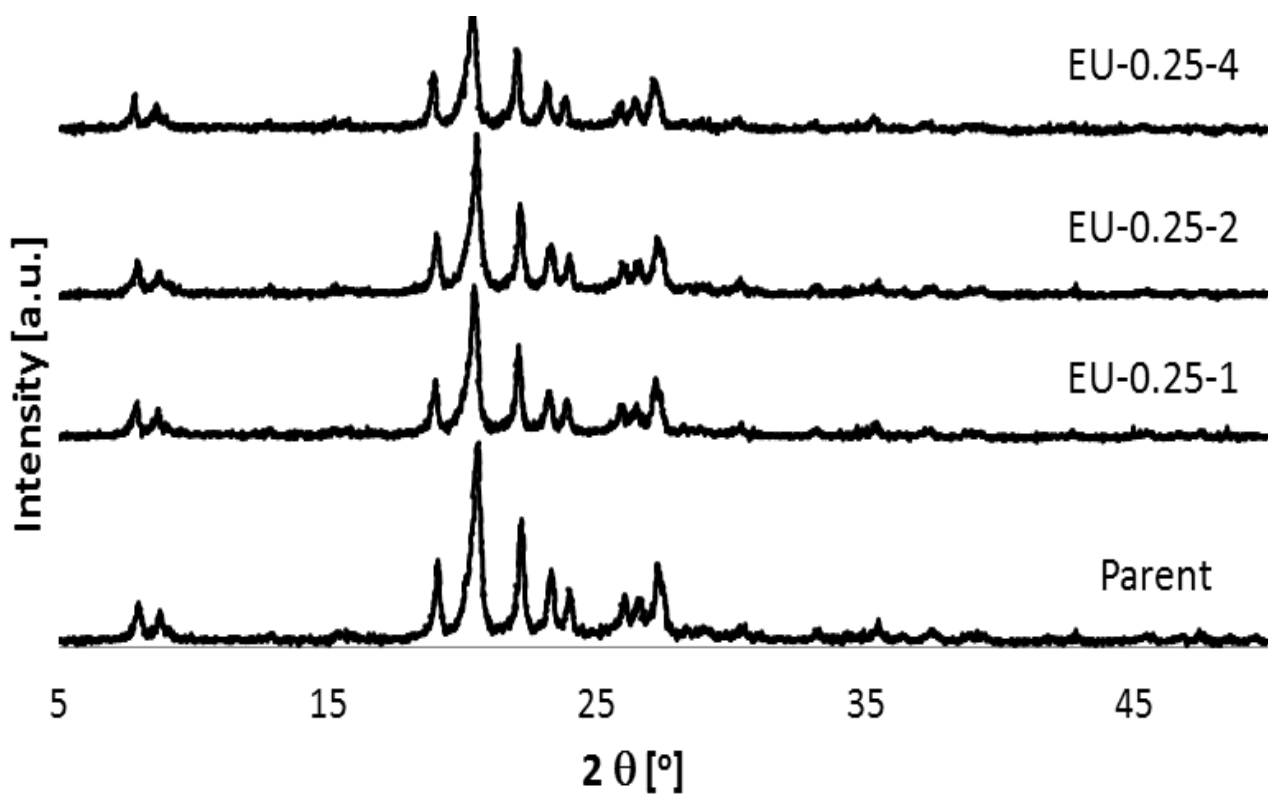
Figure 25: XRD patterns of parent and desilicated EU-1 samples at different HNO$_3$ concentrations.

Table 9: Crystallinity of treated samples with different alkaline and acid concentrations as a percentage of parent sample

Alkaline Concentration (M)	Crystallinity (%)			
	Acid Concentration (M)			
	Non-acid treated	**1**	**2**	**4**
0.25	82.9	84.7	83.3	82.8
0.5	57.8	83.6	82.3	83.1
0.75	56.9	83	82.1	81.2

5.10 Effect of sequential treatment on EU-1 morphology

The effect of acid treatment on the desilicated EU-1 samples was observed clearly using SEM micrographs, the shape of the crystals on the surface of the agglomerated particle was very determined comparing with the sample only desilicated. In Figure 26,the effect of different NaOH concentrations and fixed HNO_3 concentration on the size of created mesopores was also noted and confirmed our previous finding that increasing the NaOH concentration will increase the size of the created pores. The effect of different HNO_3 concentrations determined the degree of cleaning or removing the Al species as shown in Figure 27 and Figure 28.
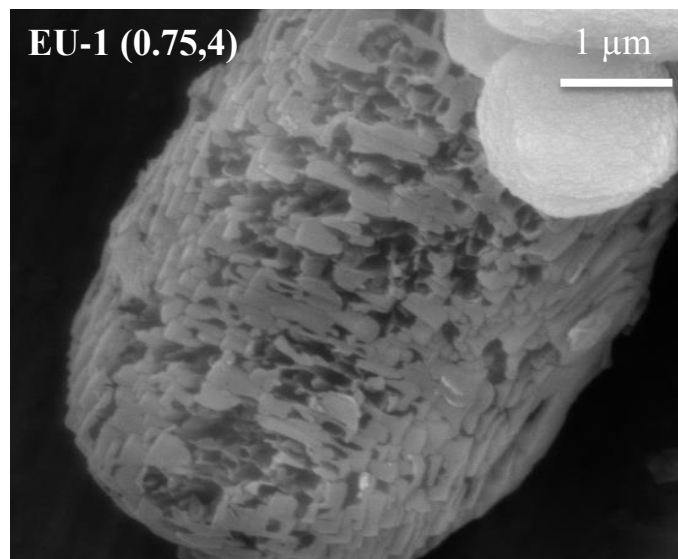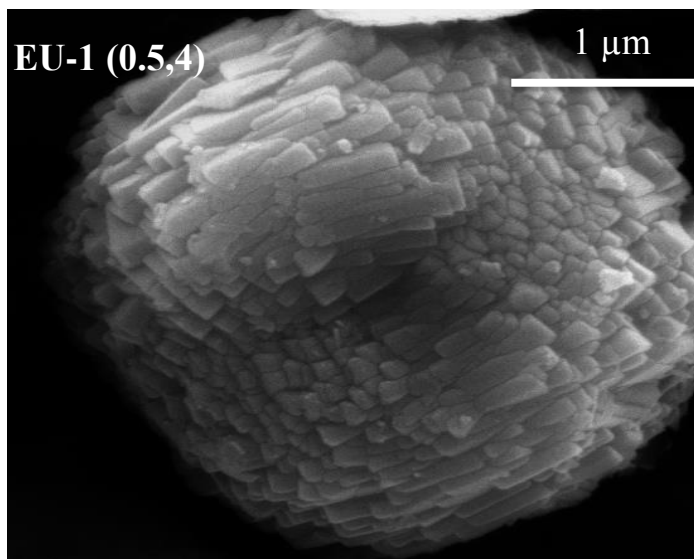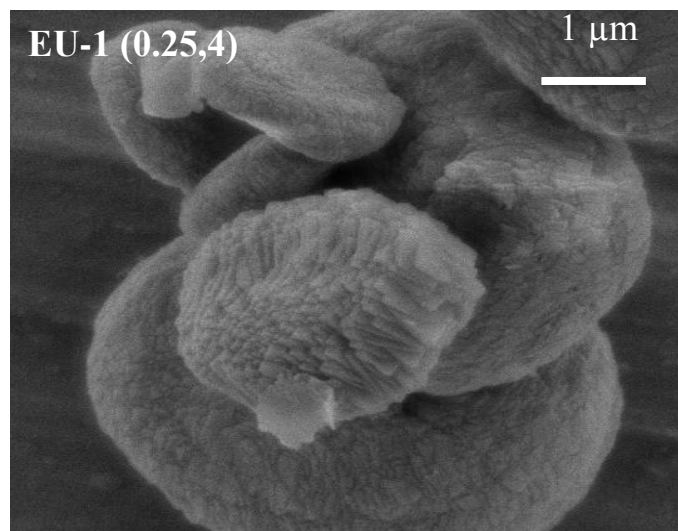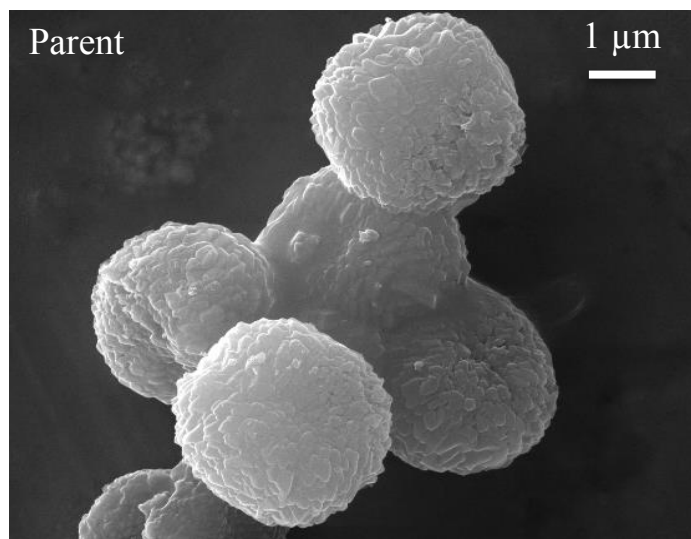
Figure 26: SEM images for parent and treated samples with 4 M HNO$_3$ and different NaOH concentrations.
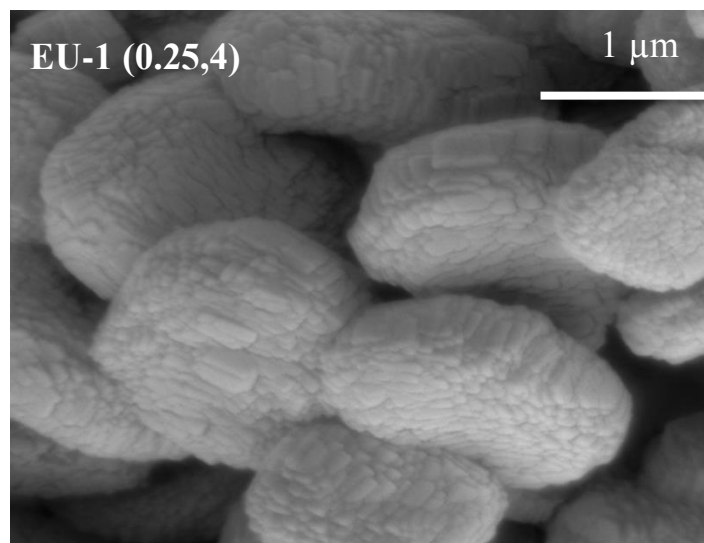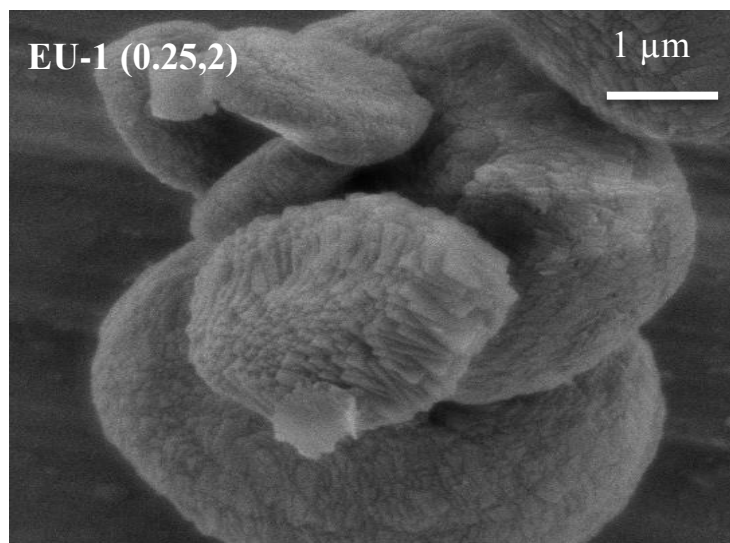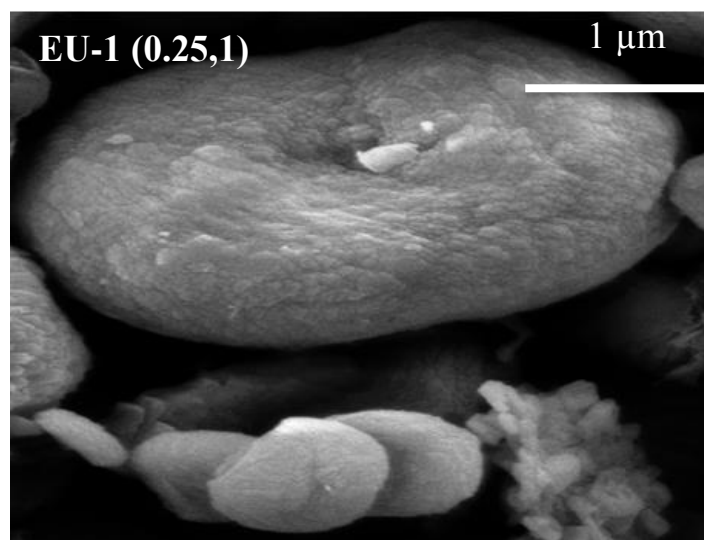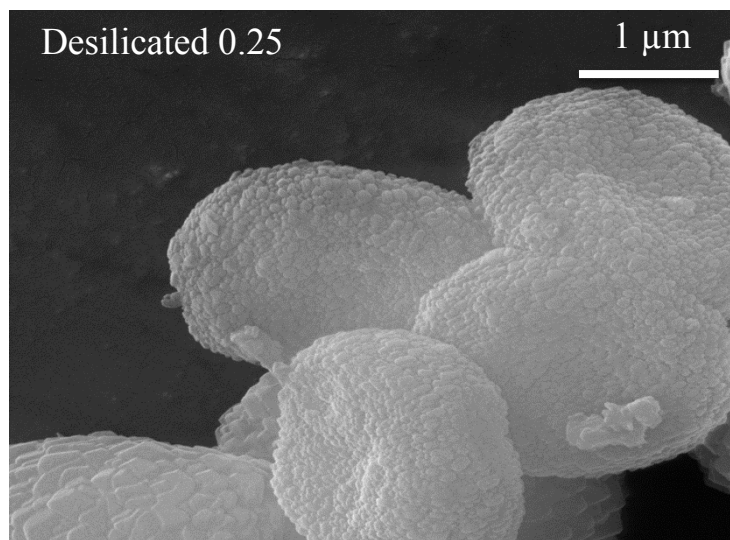
Figure 27: SEM images for parent and treated samples with 0.25 M NaOH and different HNO$_3$ concentrations
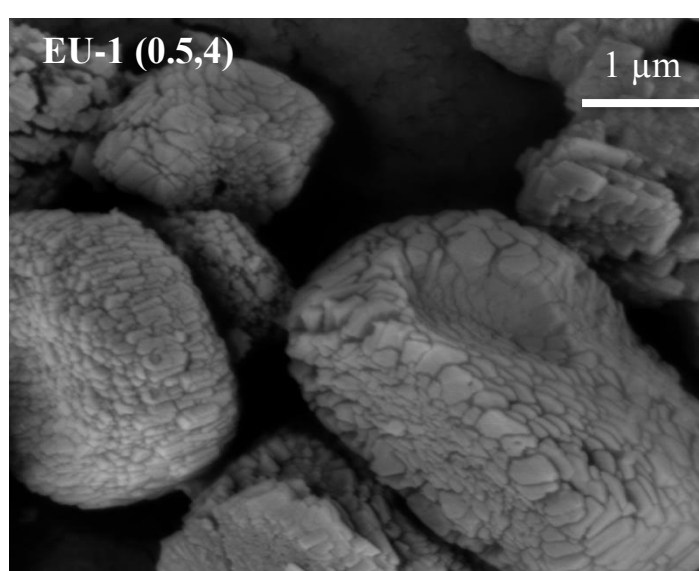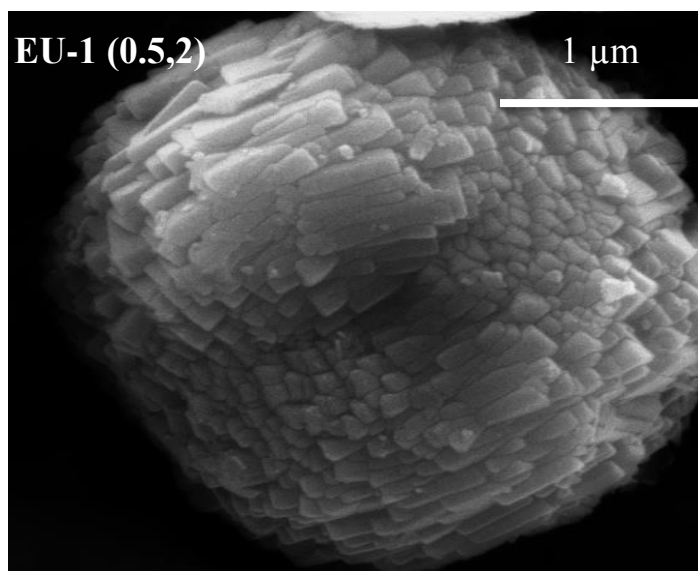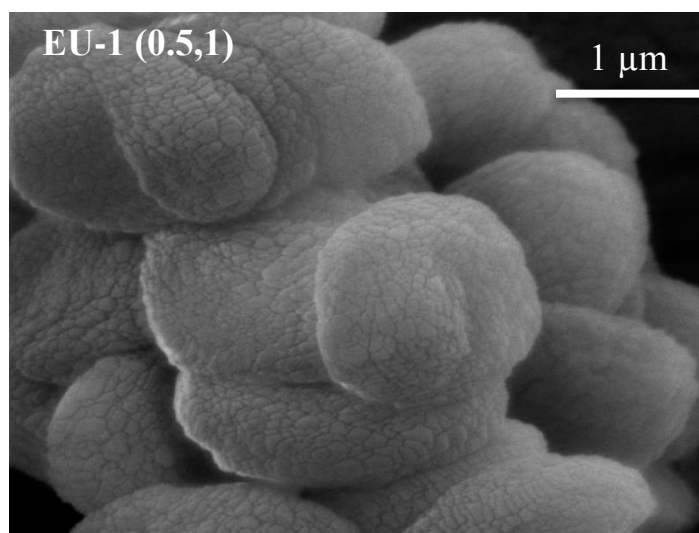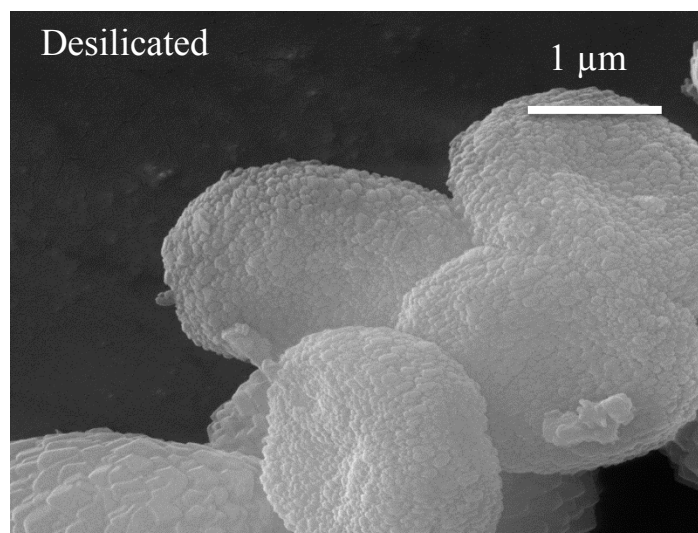
Figure 28: SEM images for parent and treated samples with 0. 5 M NaOH and different HNO$_3$ concentrations.

5.11 Effect of sequential treatment on EU-1 Si/Al

Elementary composition of the treated samples was determined by EDX technique. EU-1 synthesized crystals with 25 Si/Al ratio were treated to develop hierarchical structure. The effect of NaOH concentration was discussed before in our previous work and the minimum Si/Al achieved was 14.1 using 0.5 M of NaOH. However, applying the acid treatment increased the Si/Al ratio again because of removing of framework and non-framework Al species as reported for ZSM-22 (TON) elsewhere [70]. Changing the acid concentration from 1 M to 4 M did not make wide increment in Si/Al ratio. This can be explained that using 1 M of HNO_3 acid was enough to remove all outer (non-framework) Al species, furthermore increasing in HNO_3 concentration extracted some framework together with non- framework Al species. The samples desilicated with 0.5 M of NaOH still have the minimum Si/Al after the dealumintion with HNO_3 acid comparing with other NaOH concentrations in the same condition.

Table 10: Si/Al ratio of treated samples with different alkaline and acid concentrations

Alkaline Concentration (M)	Acid Concentration (M)		
	Non-acid treated	1	4
0.25	16.7	24.1	24.5
0.5	14.1	19.4	19.9
0.75	15.8	21.1	21.6

5.12 Effect of post-synthesis treatments on the textural properties of EU-1

The non-framework Al species are easily to be extracted especially after alkaline treatment because it's not well connected to the crystal structure. EU-1(0.25, 4) sample recovered 101.1% of its original microporosity surface area after treatment by 4 M of HNO_3 because of removing of these Al species. However, increasing the NaOH concentration to 0.5 M with the same concentration of HNO_3 increased the recovery ratio to 101.6% and that due to more accessibility to blocked pores. However, harsh alkaline treatment with 0.75 M of NaOH followed by 4 M of HNO_3 reduced the recovery ratio to 94.3% and this because of crystal dissolution which has been observed in the yield results. Regarding the mesoporosity surface area, as reported in our previous work some of the existed and the created mesoporosity was blocked by Al species. When the samples treated with HON_3, all the existed mesoporosity were recovered. Moreover, the created mesoporosity were becoming more accessible and a good increasing was observed. The mesoporosity surface area of EU-1(0.25, 4) sample was increased by 11% as compared with the parent sample and 32% as compared with the desilicated sample. EU-1(0.5, 4) showed higher increasing of 15.5% comparing with parent and 143% comparing with the desilicated sample. EU-1(0.75, 4) showed the highest increasing of 21% comparing with parent sample and 179% comparing with the desilicated sample. These increments in the microporosity and the mesoporosity surface area after acid treatment confirmed the scenario of deposited Al species on the outer pores.

Consequently, the micropore volume increased from 0.088 to 0.106 cm^3/g for both EU-1(0.25, 4) and EU-1(0.5, 4) samples and to 0.099 cm^3/g for EU-1(0.75, 4) sample. Similarly, the mesopore volume increased with the increase of NaOH concentration and the highest mesopore volume reported is 0.108 cm^3/g for EU-1(0.75, 4) sample. Actually this very reasonable because

increasing the NaOH concentration will give a chance to create more mesoporosity. Figure 28. Shows the ploting of pore volume at different ratio of (P/P_0).

The pore size distributions were determined using BJH calculations. The results showed good agreement with the BET results for mesoporosity. For all NaOH concentrations followed by acid treatment there were an increasing in the mesoporosity in comparing with the parent sample noted in the BHJ chart in Figure 29. The effect of sequential alkaline and acid treatments was clearly observed in term of size distribution when we compare with the previous desilicaion results. As the NaOH increased, the quantity and the size of the mesopores increased.

Table 11: Textural properties of parent and treated samples with different alkaline concentrations and fixed acid concentration.

Sample	S_{total} (m^2/g)	S_{micro} (m^2/g)	S_{meso} (m^2/g)	V_{micro} (cm^3/g)	V_{meso} (cm^3/g)
Parent	277.0	225.5	51.5	0.088	0.078
EU-1(0.25, 0)	246.1	202.8	43.4	0.079	0.081
EU-1(0.25, 4)	285.4	228	57.4	0.106	0.082
EU-1(0.5, 0)	139.4	113.9	24.5	0.044	0.048
EU-1(0.5, 4)	288.7	229.2	59.5	0.106	0.084
EU-1(0.75,0)	128.9	104.5	22.4	0.041	0.046
EU-1(0.75, 4)	275.2	212.7	62.5	0.099	0.108
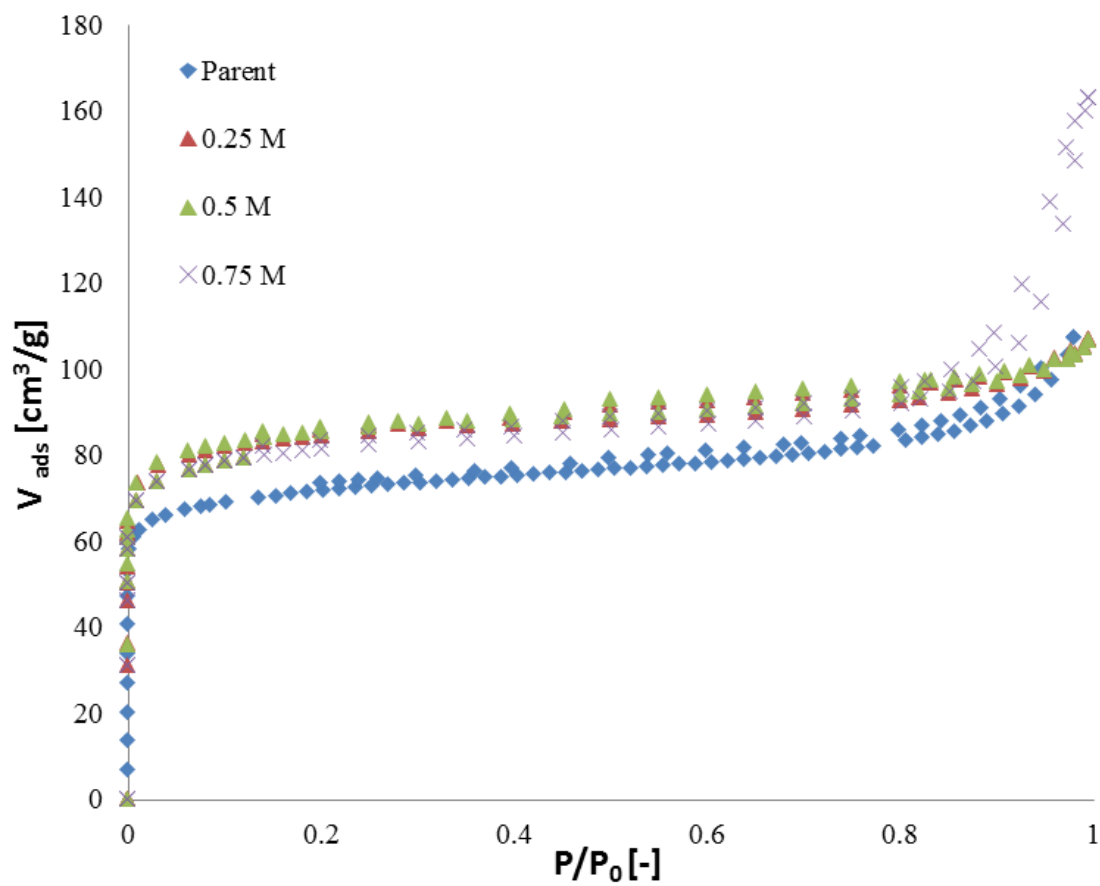
Figure 29: Isotherms plot for N$_2$ adsorption and desorption of parent and treated samples at fixed HNO$_3$ concentration (4 M).
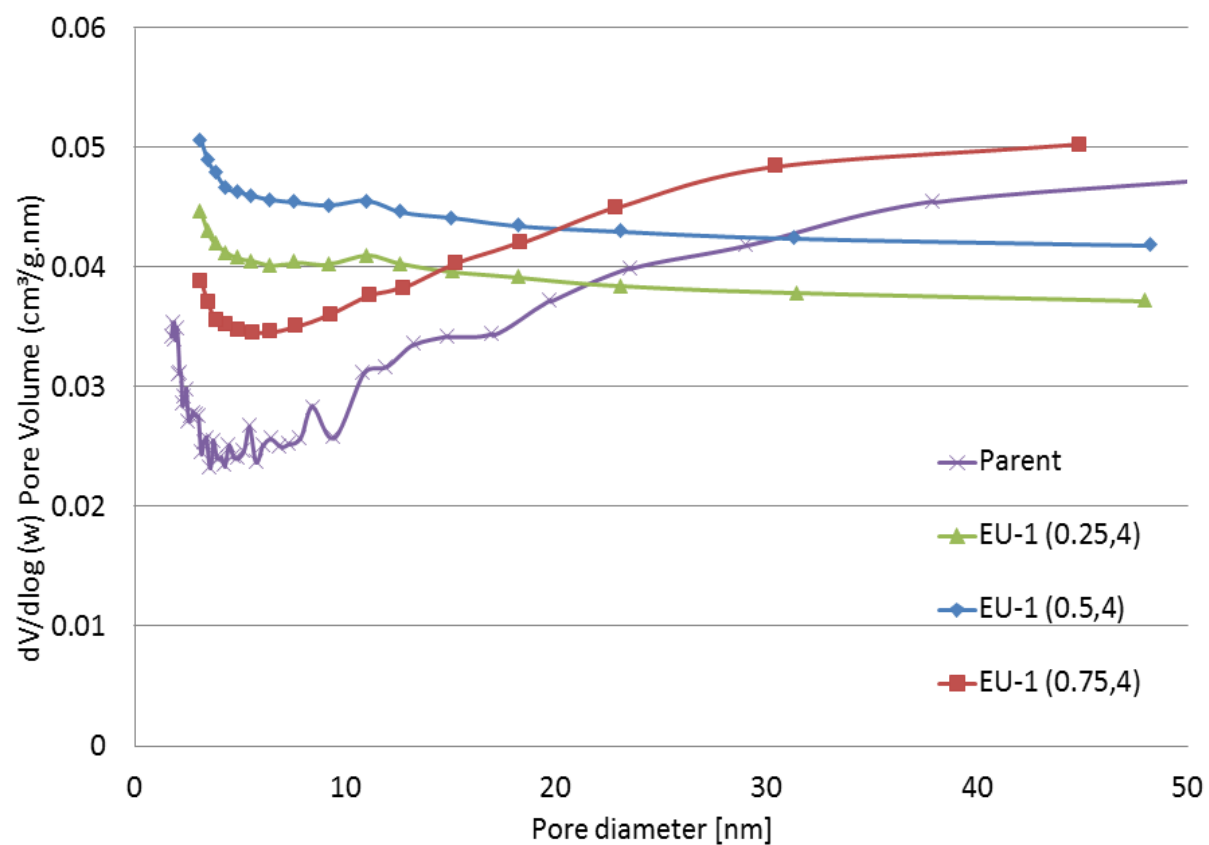
Figure 30: BJH mesopore size distribution of parent and desilicated EU-1 samples for 60 min.

5.13 Effect of sequential treatments on EU-1 acidity

Ammonia temperature programmed desorption (NH_3-TPD) was performed to test the effect of different alkaline and acid treatment concentrations on EU-1 acidity. The TPD measurements were applied in the range of 200-600 ^oC with a heating rate of 10 ^oC min^{-1}. The all samples showed mainly two peaks at 303 and 500 ^oC as shown in Figure 31 and Figure 32 related to weak and strong acid sites respectively as reported elsewhere by Martins et. al [89].

5.13.1 Effect of alkaline concentration at fixed acid concentration

Applying the acid treatment after alkaline treatment gave a good increasing in the amount of desorbed ammonia (total acidity) comparing with non-acid treated samples which showed large decreasing. 2 M concentration of HNO_3 used to treat the samples after it was treated with different NaOH concentrations. An increasing in the total acidity was observed for the samples treated with 0.25 and 0.5 M of NaOH, which indicate that removing of non-framework Al species which deposited and blocked the pores which gave more accessibility to extra acid active sites as plotted in Figure 31. But for the case of 0.75 M treatment we noted a decreasing on the acidity, this decreasing confirms removing of large amount of non-framework Al species which existed because of highly concentrated alkaline treatment which also has a destructive impact on the zeolite crystals and[90].

5.13.2 Effect of acid concentration at fixed mild alkaline concentration

A relatively mild concentration of NaOH (0.25 M) followed by two different concentrations of HNO_3 (2 and 4) were used to study the effect on the EU-1 zeolite acidity. Based on our previous discussion for the case of alkaline treatment only, we reported the decreasing on acidity due to

deposition of Al species on the EU-1 pores. These Al species removed easily by acid treatment, using 2 M concentration of HNO_3 showed a good increasing in the acidity and furthermore increasing on HNO_3 concentration to 4 M gave little increasing, this because higher concentration will facilitate to remove more non-framework Al species which blocked the pores.

Table 12: Total acidity of parent and treated samples as calculated from NH$_3$ desorption results

Sample	NH$_3$-TPD(mmol/g)
Parent	0.273
EU-1 (0.25,2)	0.472
EU-1 (0.5,2)	0.523
EU-1 (0.75,2)	0.260
EU-1 (0.25,4)	0.494
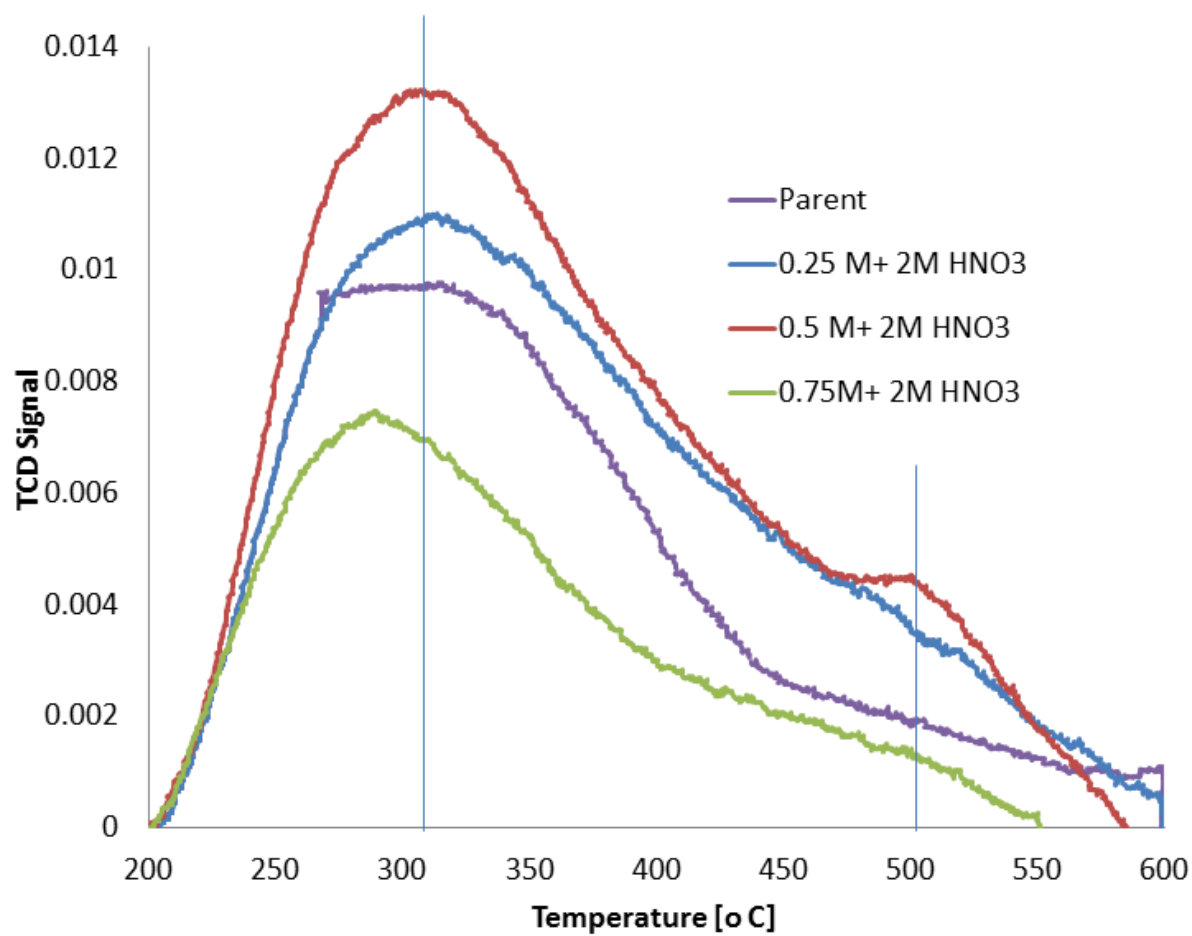
Figure 31: NH3-TPD profiles of EU-1 desilicated samples for 60 min.
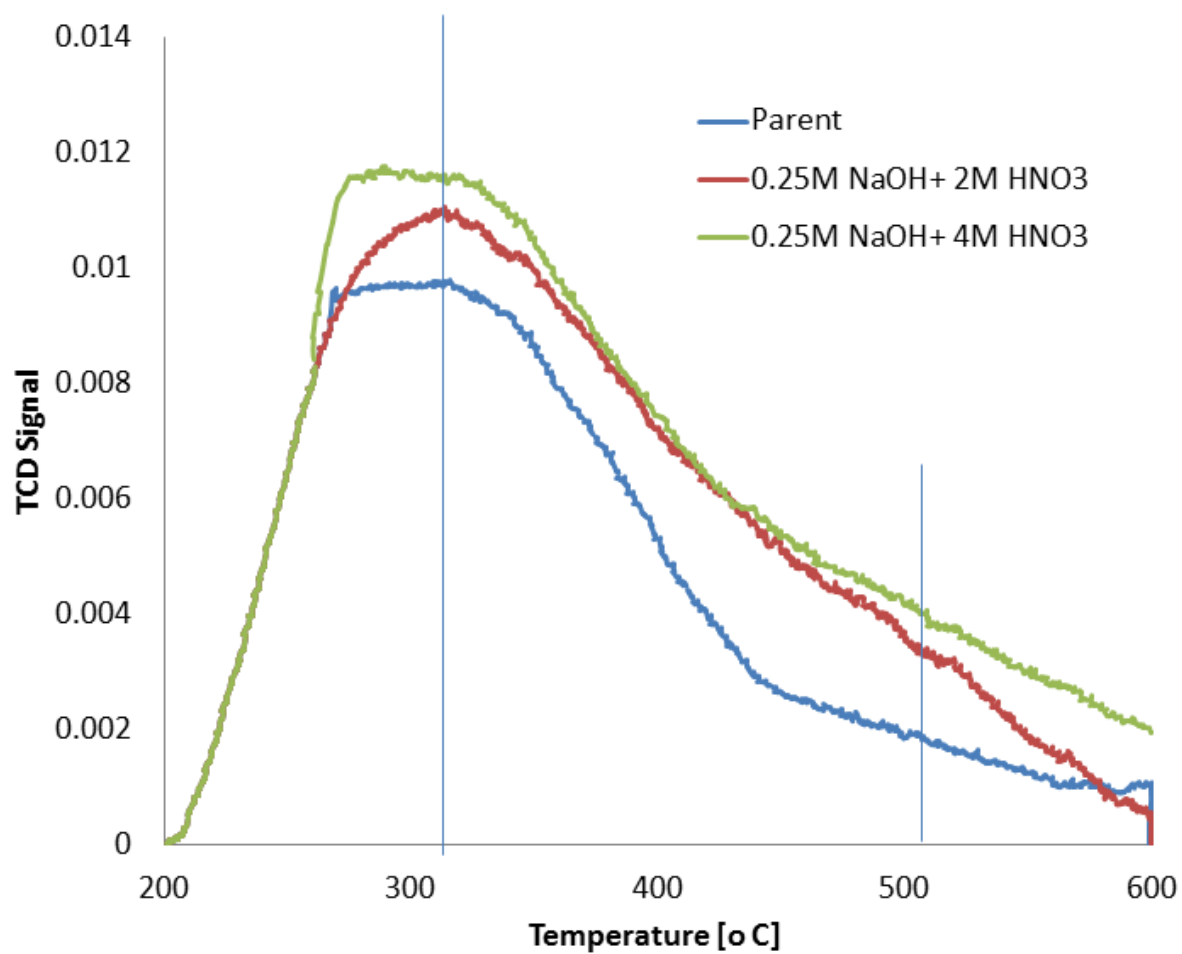
Figure 32: NH3-TPD profiles of EU-1 desilicated samples for 60 min.

5.14 Evaluation of hierarchical EU-1 samples on dimethyl ether conversion

The previous results of desilicated samples showed a lower catalytic activity comparing with the parent samples. These results were attributed to loose of microporosity which is holding the active sites. The BET and NH_3-TPD results confirmed an inordinate decreasing in the both microporosity and mesoporosity.

However, after sequential alkaline and acid treatment a good increment in term of conversion of DME to hydrocarbons was observed. EU-1 (0.5,4) recorded the highest conversion among the other tested samples. The conversion rate boosted from 19% for the desilicated sample (0.5 M of NaOH) to 48.4% in the case of the both treatment together comparing with 37% in the case of the parent sample. Furthermore, the selectivity toward propylene (C3=) recorded the highest production among other products which reached to 24% (quarter of the converted DME amount) comparing with 11% in the case of parent and desilicated sample. These results can be directly linked to the previous characterization results which showed that EU-1 (0.5,4) has the highest microporosity surface area and micropore volume together with the highest concentration of the acid sites.

Similarly, EU-1 (0.75,4) showed large increasing in term of conversion from 12% in the case of desilicated sample (0.75 M of NaOH) to 29% after acid treatment but it's still below the conversion of the parent sample which was 37%. Unfortunately, the destructive effect of using high concentrated alkaline yielded to lose some microporosity and that was clear in the results of surface area and acidity. The relatively large amount of created mesoporosity boosted the selectivity of propylene for 0.5% up to 23% and this another indication confirms that the distinctive structure of hierarchical EU-1 succeed to be selective toward propylene. The

recovered microporosity increased the ethylene selectivity from 2% to 12% as presented in Table

13. and Figure 33.

Regarding the selectivity of propylene over ethylene (P/E), this ratio reached up to 2.4 in the case

of desilicated sample (0.5 M of NaOH) because the blocking of the microporosity eliminated the

formation of ethylene. However, when the micorporosity was recovered and increased after acid

treatment this ration decreased to 2.1. Generally, it observed that creating more mesoporosity

favored the formation of propylene over other hydrocarbons in the case of dimethyl ether

conversion.

Another good achievement of the hierarchical structure, EU-1 (EUO) showed in previous work

reported by Teketel et. al [21] for methanol to hydrocarbons the selectivity of EU-1 to the

aromatics products especially at low conversion. He explained that by the topology of EU-1 and

diffusion limitation because of narrowing of 10-ring channels to 12-ringside pockets. This

problem overpassed by the hierarchical design of EU-1 which lowered the aromatic selectivity to

less than 10% in the case of EU-1 (0.5,4) sample. Figure 33 and Figure 34 represent the

conversion of DME and the selectivity for all the products over all the treated samples.

Table 13: Conversion and selectivity of DME over parent and hierarchical EU-1 zeolite

Samples	Conversion	C2=	C3=	P/E ratio
Parent	37	5.8	11.1	1.9
EU-1 (0.5,0)	19	4.6	11.3	2.4
EU-1 (0.5,4)	48	11.7	24.2	2.1
EU-1 (0.75,0)	12	2.1	0.5	-
EU-1 (0.75,4)	29	12.4	23.2	1.8
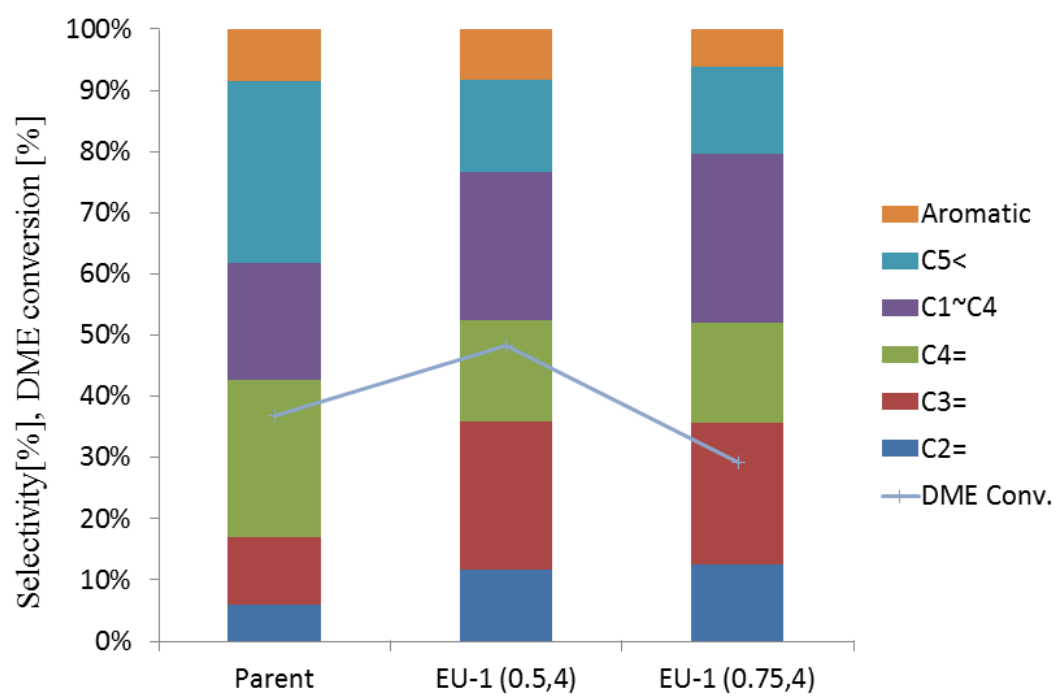
Figure 33: DME to olefins reaction results for parent and sequential treated samples for 60 min.
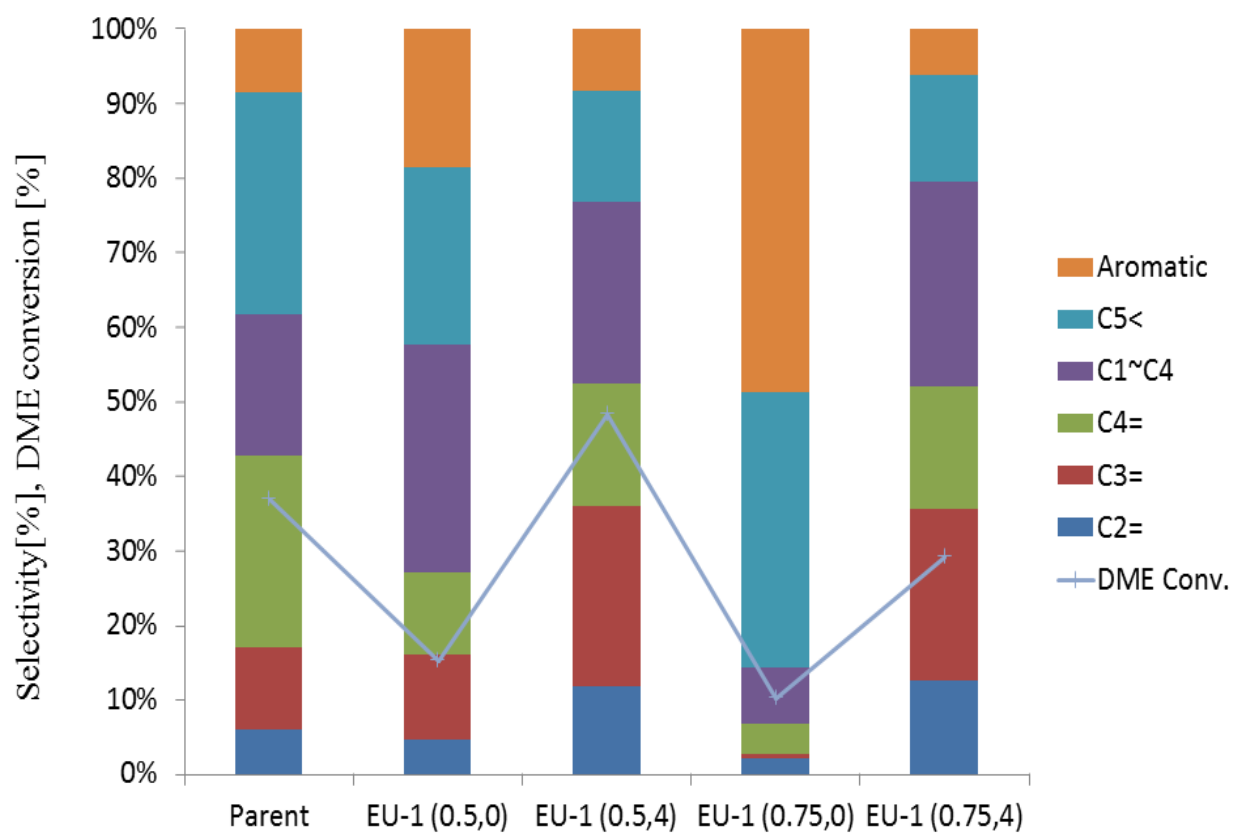
Figure 34: DME to olefins reaction results for parent and alkaline and alkaline acid treated samples for 60 min.

5.15 Calculations of effective diffusivity for sequentially treated samples

$$D_{eff} = \frac{D_{AB}\emptyset_P\sigma_c}{\tau}$$

Where

$$\emptyset_P = Pellet\ porosity = \frac{Volume\ of\ void\ space}{Total\ volume\ (Voids\ and\ solids)}$$

$$\sigma_c = constriction\ factor$$

$$\tau = Tortusity = \frac{Actual\ distance\ a\ molecule\ travels\ between\ two\ points}{Shortest\ distance\ between\ those\ two\ points}$$

Assumptions:

- As EU-1 has straight channels so $\tau = 1$.

- As there is no variation in the cross-sectional area in EU-1 channels $\sigma_c = 1$.

There for:

$$D_{eff} = D_{AB}\emptyset_P$$

$$D_{AB} = D_o e^{(-\frac{E}{RT})}$$

Given

D_{AB} (T=298) = 1.2 *10^{-9} cm^2/s $\qquad\qquad$ D_{AB} (T=313) = 1.5 *10^{-9} cm^2/s

After calculations

D_o = 3.95 *10^{-8} cm^2/s $\qquad\qquad$ E= 8.51*10^3 kJ/mol

D_{AB} (T=623) = 7.6 *10^{-9} cm^2/s

Zeolite density= 1.06 g/cm^3

For the base of 1 g of EU-1 zeolite $\qquad\qquad$ V= 0.943 cm^3

Sample name	Total pore volume (Cm^3/g)	Pellet porosity (-)	D_{eff} at T=298K (cm^2/s)	D_{eff} at T=623K (cm^2/s)
Parent	0.166	0.176	2.1*10^{-10}	1.3*10^{-9}
EU-1 (0.25-4)	0.188	0.200	2.4*10^{-10}	1.5*10^{-9}
EU-1 (0.5-4)	0.190	0.201	2.4*10^{-10}	1.5*10^{-9}
EU-1 (0.75-4)	0.207	0.220	2.6*10^{-10}	1.7*10^{-9}

CHAPTER 6

CONCLUSIONS

The small synthesis window of EU-1 was observed as the synthesis was very sensitive to the synthesis parameters. The highest crystallinity has been found at 12 h aging time. Further increase of aging time to 24 h induced the appearance of impurity phases. The temperature was also crucial parameter. Slight change in temperature reduced the crystallinity of EU-1. It has been found that temperature of 190 $^{\circ}$C provided the optimum crystallinity. Changing the temperature by ± 5 degrees will affect either crystallinity or morphology. XRD results confirmed that the minimum time to obtain crystalline EU-1 was 72 h. These findings provide a better platform in EU-1 synthesis, in addition to other possible modifications such as desilication and dealumination.

Treatment of EU-1 zeolite with different concentration of NaOH showed a different trend compared with other previous work in different other framework such as MFI and BEA. The behavior of EU-1 was similar to previous reports on ZSM-22 as both zeolites are representing one dimensional channel with rod-like crystals. The formation of mesoporosity was confirmed by TEM and porosity analysis of EU-1. The deposition of Al species on the zeolite surface during alkaline treatment called 'realumination' explained the unexpected results like the decreasing in the mesopore surface area and the pore volume. It was found that the minimum achievable Si/Al ratio was 14 with 0.5 M NaOH for 60 min. However, on the other side increasing the treatment concentration led to the formation of large pores, which are known as macroporosity. The reaction of DME to olefins over desilicated samples showed decreases in conversion due to the destruction of some microporosity, which holds the active Brønsted acid site. The appearance of mesopores increased the selectivity toward propylene, which is the

preferred olefin currently in the market . However, the further increase in concentration of NaOH induced the formation of macroporosity, which has lower selectivity to propylene. Macroporosity also favored selectivity to heavy products such as aromatics. In order to remove the deposited Al-species, it is recommended to apply additional dealumination, either by acid or steam treatment to recover the lost microporosity and acid sites.

The acid treatment achieved the required objectives of recovering the blocked microporosity of the desilicated samples. Moreover, it helped to clean the created mesoporosity from the deposited Al species and facilitate the diffusion of reactants and products through the particles. XRD results show an increasing crystallinity for the acid treated samples over the desilicated samples because of removing of the amorphous phase of Al which is located on the outer surface. Furthermore, large increase in the mesoporosity reported after the acid treatment together with an increase in the acidity for the samples treated with 0.25 and 0.5 M of NaOH.

The EU-1 (0.5,4) presents the best results in terms of BET surface area and total acidity. Consequently, it shows the best performance in converting dimethyl ether to propylene. The availability of more active acid sites combined with better mass transfer performance increased the conversion of dimethyl ether to olefins from 37 to 48% in the case of EU-1 (0.5,4) sample. The characteristic design of the hierarchical EU-1 zeolite enhanced the selectivity of propylene over other products which reached to 24%.in the best case. It was also observed that, creating more mesoporosity with preserving the microporosity which holds the active sites will give better catalytic performance. Treatment time and alkaline concentration have some limitations in creating more mesoporosity. The possible solution to create more msoporosity is to apply multiple alkaline treatments followed by acid treatment to remove any amount of deposited Al.

Succeeding in this step will remove a lot of restrictions on using of one-dimension zeolites in many catalytic processes.

References

1. Casci, J.L., B.M. Lowe, and T.V. Whittam, *Zeolite EU-1 and a method of making zeolite EU-1*. 1985, Google Patents.

2. Briscoe, N., et al., *The framework topology of zeolite EU-1*. Zeolites, 1988. **8**(1): p. 74-76.

3. Giordano, G., J. Nagy, and E. Derouane, *Zeolite synthesis in presence of hexamethonium ions*. Journal of Molecular Catalysis A: Chemical, 2009. **305**(1): p. 34-39.

4. Liu, X., U. Ravon, and A. Tuel, *Synthesis of all-silica zeolites from highly concentrated gels containing hexamethonium cations*. Microporous and Mesoporous Materials, 2012. **156**: p. 257-261.

5. Rao, G., et al., *Synthesis and characterization of high-silica EU-1*. Zeolites, 1989. **9**(6): p. 483-490.

6. Xu, Q., et al., *Synthesis of high-silica EU-1 zeolite in the presence of hexamethonium ions: a seeded approach for inhibiting ZSM-48*. Journal of colloid and interface science, 2011. **358**(1): p. 252-260.

7. Moini, A., et al., *The role of diquaternary cations as directing agents in zeolite synthesis*. Zeolites, 1994. **14**(7): p. 504-511.

8. Matias, P., et al., *Desilication of a TON zeolite with NaOH: Influence on porosity, acidity and catalytic properties*. Applied Catalysis A: General, 2011. **399**(1): p. 100-109.

9. Wang, Y.W.S., *Hierarchical Zeolites: Synthesis and Applications in Bioenergy*.

10. van Laak, A.N., et al., *Mesoporous mordenites obtained by sequential acid and alkaline treatments–Catalysts for cumene production with enhanced accessibility*. Journal of Catalysis, 2010. **276**(1): p. 170-180.

11. Sá Couto, C., et al., *Towards a Deep Desilication/Dealumination of NU‐10 Zeolite: Shape‐Selectivity Regulation*. European Journal of Inorganic Chemistry, 2012. **2012**(26): p. 4190-4199.

12. Tao, Y., et al., *Mesopore-modified zeolites: preparation, characterization, and applications*. Chemical reviews, 2006. **106**(3): p. 896-910.

13. Schmidt, I., C. Madsen, and C.J. Jacobsen, *Confined space synthesis. A novel route to nanosized zeolites.* Inorganic chemistry, 2000. **39**(11): p. 2279-2283.

14. Mintova, S., J.-P. Gilson, and V. Valtchev, *Advances in nanosized zeolites.* Nanoscale, 2013. **5**(15): p. 6693-6703.

15. Covarrubias, C., R. Quijada, and R. Rojas, *Synthesis of nanosized ZSM-2 zeolite with potential acid catalytic properties.* Microporous and Mesoporous Materials, 2009. **117**(1–2): p. 118-125.

16. Larlus, O., S. Mintova, and T. Bein, *Environmental syntheses of nanosized zeolites with high yield and monomodal particle size distribution.* Microporous and Mesoporous Materials, 2006. **96**(1–3): p. 405-412.

17. Chen, F., et al., *Synthesis of hierarchical porous zeolite and its performance in n-heptane cracking.* Catalysis Communications, 2012. **18**(0): p. 110-114.

18. Muraza, O., et al., *Selective catalytic cracking of n-hexane to propylene over hierarchical MTT zeolite.* Fuel, 2014. **135**(0): p. 105-111.

19. Zheng, J., et al., *The hierarchical effects of zeolite composites in catalysis.* Catalysis Today, 2011. **168**(1): p. 124-132.

20. Tarach, K., et al., *Catalytic cracking performance of alkaline-treated zeolite Beta in the terms of acid sites properties and their accessibility.* Journal of Catalysis, 2014. **312**(0): p. 46-57.

21. Teketel, S., et al., *Shape selectivity in the conversion of methanol to hydrocarbons: the catalytic performance of one-dimensional 10-ring zeolites: ZSM-22, ZSM-23, ZSM-48, and EU-1.* ACS Catalysis, 2011. **2**(1): p. 26-37.

22. Hu, S., et al., *Highly selective formation of propylene from methanol over high-silica EU-1 zeolite catalyst.* Catalysis Communications, 2012. **28**: p. 95-99.

23. Cejka, J., A. Corma, and S. Zones, *Zeolites and catalysis: synthesis, reactions and applications*. 2010: John Wiley & Sons.

24. Pham-Huu, C., et al., *BETA zeolite nanowire synthesis under non-hydrothermal conditions using carbon nanotubes as template.* Carbon, 2004. **42**(10): p. 1941-1946.

25. Larsen, S.C., *Nanocrystalline zeolites and zeolite structures: synthesis, characterization, and applications.* The Journal of Physical Chemistry C, 2007. **111**(50): p. 18464-18474.

26.   Tosheva, L. and V.P. Valtchev, *Nanozeolites: synthesis, crystallization mechanism, and applications.* Chemistry of Materials, 2005. **17**(10): p. 2494-2513.

27.   Wang, J., et al., *TUD-C: A tunable, hierarchically structured mesoporous zeolite composite.* Microporous and Mesoporous Materials, 2009. **120**(1–2): p. 19-28.

28.   Serrano, D. and P. Pizarro, *Synthesis strategies in the search for hierarchical zeolites.* Chemical Society Reviews, 2013. **42**(9): p. 4004-4035.

29.   Chen, L.-H., et al., *Hierarchically structured zeolites: synthesis, mass transport properties and applications.* Journal of Materials Chemistry, 2012. **22**(34): p. 17381-17403.

30.   Groen, J.C., J.A. Moulijn, and J. Pérez-Ramírez, *Desilication: on the controlled generation of mesoporosity in MFI zeolites.* Journal of Materials Chemistry, 2006. **16**(22): p. 2121-2131.

31.   Groen, J.C., J.A. Moulijn, and J. Pérez-Ramírez, *Decoupling mesoporosity formation and acidity modification in ZSM-5 zeolites by sequential desilication–dealumination.* Microporous and mesoporous materials, 2005. **87**(2): p. 153-161.

32.   Yang, X.-Y., et al., *Self-formation phenomenon to hierarchically structured porous materials: design, synthesis, formation mechanism and applications.* Chemical Communications, 2011. **47**(10): p. 2763-2786.

33.   Tan, Q., et al., *Synthesis, characterization, and catalytic properties of hydrothermally stable macro–meso–micro-porous composite materials synthesized via in situ assembly of preformed zeolite Y nanoclusters on kaolin.* Journal of Catalysis, 2007. **251**(1): p. 69-79.

34.   Cui, Y., et al., *Pore-structure-mediated hierarchical SAPO-34: Facile synthesis, tunable nanostructure, and catalysis applications for the conversion of dimethyl ether into olefins.* Particuology, 2013. **11**(4): p. 468-474.

35.   Li, X.S., et al., *Templating mesoporous hierarchies in silica thin films using the thermal degradation of cellulose nitrate.* Microporous and Mesoporous Materials, 2007. **99**(3): p. 308-318.

36.   Verboekend, D. and J. Pérez-Ramírez, *Design of hierarchical zeolite catalysts by desilication.* Catalysis Science & Technology, 2011. **1**(6): p. 879-890.

37. Sadowska, K., K. Góra-Marek, and J. Datka, *Hierarchic zeolites studied by IR spectroscopy: Acid properties of zeolite ZSM-5 desilicated with NaOH and NaOH/tetrabutylamine hydroxide.* Vibrational Spectroscopy, 2012. **63**: p. 418-425.

38. Silaghi, M.-C., C. Chizallet, and P. Raybaud, *Challenges on molecular aspects of dealumination and desilication of zeolites.* Microporous and Mesoporous Materials, 2014. **191**: p. 82-96.

39. Sardesai, A. and S. Lee, *Alternative source of propylene.* Energy sources, 2005. **27**(6): p. 489-500.

40. Sardesai, A. and S. Lee. *Hydrocarbon synthesis from dimethyl ether over ZSM-5 catalyst.* in *ABSTRACTS OF PAPERS OF THE AMERICAN CHEMICAL SOCIETY*. 1998. AMER CHEMICAL SOC 1155 16TH ST, NW, WASHINGTON, DC 20036 USA.

41. Cai, G., et al., *Light alkenes from syngas via dimethyl ether.* Applied Catalysis A: General, 1995. **125**(1): p. 29-38.

42. Liu, Z., et al., *Research progress and pilot plant test on SDTO process.* Studies in surface science and catalysis, 1998. **119**: p. 895-900.

43. Biryukova, E., et al., *Conversion of dimethyl ether into lower olefins on a La-Zr-HZSM-5/Al2O3 zeolite catalyst.* Petroleum Chemistry, 2011. **51**(1): p. 49-54.

44. Kolesnichenko, N., et al., *Conversion of dimethyl ether into C2-C4 olefins on zeolite catalysts.* Petroleum Chemistry, 2009. **49**(1): p. 42-46.

45. Li, Y., et al., *Differences in the methanol-to-olefins reaction catalyzed by SAPO-34 with dimethyl ether as reactant.* Journal of Catalysis, 2014. **311**: p. 281-287.

46. Al-Dughaither, A.S. and H. de Lasa, *Neat dimethyl ether conversion to olefins (DTO) over HZSM-5: Effect of SiO2/Al2O3 on porosity, surface chemistry, and reactivity.* Fuel, 2014. **138**(0): p. 52-64.

47. Abramova, A., *Development of catalysts based on pentasil-type zeolites for selective synthesis of lower olefins from methanol and dimethyl ether.* Catalysis in Industry, 2009. **1**(4): p. 267-277.

48. Hu, S., et al., *Highly selective formation of propylene from methanol over high-silica EU-1 zeolite catalyst.* Catalysis Communications, 2012.

49. Zhao, T.-S., T. Takemoto, and N. Tsubaki, *Direct synthesis of propylene and light olefins from dimethyl ether catalyzed by modified H-ZSM-5.* Catalysis Communications, 2006. **7**(9): p. 647-650.

50. Kolesnichenko, N., et al., *Synthesis of lower olefins from dimethyl ether in the presence of zeolite catalysts modified with rhodium compounds.* Petroleum Chemistry, 2011. **51**(1): p. 55-60.

51. Chen, W.-H., et al., *One-step synthesis of dimethyl ether from the gas mixture containing CO< sub> 2</sub> with high space velocity.* Applied Energy, 2012. **98**: p. 92-101.

52. Rouleau, L., et al., *Process for preparing a zeolite with structure type EUO using structuring agent precursors and its use as an AC8 isomerisation catalyst.* 2002, Google Patents.

53. Rao, G. and A. Kotasthane, *Thermal and hydrothermal stabilities of zeolite EU-1.* Applied Catalysis A: General, 1994. **119**(1): p. 33-43.

54. Bats, N., et al., *Recent developments in the use of hexamethonium salts as structure directing agents in zeolite synthesis.* Studies in Surface Science and Catalysis, 2004. **154**: p. 283-288.

55. Dodwell, G.W., R. Denkewicz, and L. Sand, *Crystallization of EU—1 and EU—2 in alkali and alkali-free systems.* Zeolites, 1985. **5**(3): p. 153-157.

56. Goergen, S., et al., *Shape controlled zeolite EU-1 (EUO) catalysts: Dry gel conversion type synthesis, characterization and formation mechanisms.* Microporous and Mesoporous Materials, 2009. **126**(3): p. 283-290.

57. Arnold, A., M. Hunger, and J. Weitkamp, *Dry-gel synthesis of zeolites [Al] EU-1 and [Ga] EU-1.* Microporous and mesoporous materials, 2004. **67**(2): p. 205-213.

58. Groen, J., et al., *Mesoporosity development in ZSM-5 zeolite upon optimized desilication conditions in alkaline medium.* Colloids and Surfaces A: Physicochemical and Engineering Aspects, 2004. **241**(1): p. 53-58.

59. Groen, J., et al., *On the introduction of intracrystalline mesoporosity in zeolites upon desilication in alkaline medium.* Microporous and Mesoporous Materials, 2004. **69**(1): p. 29-34.

60. Groen, J.C., et al., *Mesoporous beta zeolite obtained by desilication.* Microporous and Mesoporous Materials, 2008. **114**(1): p. 93-102.

61. Bonilla, A., D. Baudouin, and J. Pérez-Ramírez, *Desilication of ferrierite zeolite for porosity generation and improved effectiveness in polyethylene pyrolysis.* Journal of Catalysis, 2009. **265**(2): p. 170-180.

62. Sommer, L., et al., *Mesopore formation in zeolite H-SSZ-13 by desilication with NaOH.* Microporous and Mesoporous Materials, 2010. **132**(3): p. 384-394.

63. Svelle, S., et al., *How defects and crystal morphology control the effects of desilication.* Catalysis Today, 2011. **168**(1): p. 38-47.

64. Li, J., et al., *Catalytic fast pyrolysis of biomass with mesoporous ZSM-5 zeolites prepared by desilication with NaOH solutions.* Applied Catalysis A: General, 2014. **470**: p. 115-122.

65. Bleken, F.L., et al., *Catalyst deactivation by coke formation in microporous and desilicated zeolite H-ZSM-5 during the conversion of methanol to hydrocarbons.* Journal of Catalysis, 2013. **307**: p. 62-73.

66. Kubů, M., M. Opanasenko, and M. Shamzy, *Modification of textural and acidic properties of -SVR zeolite by desilication.* Catalysis Today, 2014. **227**(0): p. 26-32.

67. Tarach, K., et al., *Catalytic cracking performance of alkaline-treated zeolite Beta in the terms of acid sites properties and their accessibility.* Journal of Catalysis, 2014. **312**: p. 46-57.

68. Biemelt, T., et al., *Hierarchical porous zeolite ZSM-58 derived by desilication and desilication re-assembly.* Microporous and Mesoporous Materials, 2014. **187**: p. 114-124.

69. Verboekend, D., et al., *Properties and functions of hierarchical ferrierite zeolites obtained by sequential post-synthesis treatments.* Chemistry of Materials, 2010. **22**(16): p. 4679-4689.

70. Verboekend, D., et al., *Mesoporous ZSM-22 zeolite obtained by desilication: peculiarities associated with crystal morphology and aluminium distribution.* CrystEngComm, 2011. **13**(10): p. 3408-3416.

71. Qin, Z., et al., *Mesoporous Y zeolite with homogeneous aluminum distribution obtained by sequential desilication–dealumination and its performance in the catalytic cracking of cumene and 1, 3, 5-triisopropylbenzene.* Journal of Catalysis, 2011. **278**(2): p. 266-275.

72. Verboekend, D., G. Vilé, and J. Pérez-Ramírez, *Hierarchical Y and USY Zeolites Designed by Post-Synthetic Strategies.* Advanced Functional Materials, 2012. **22**(5): p. 916-928.

73. Zhou, H., et al., *< i> In situ</i> synthesis of SAPO-34 crystals grown onto α-Al< sub> 2</sub> O< sub> 3</sub> sphere supports as the catalyst for the fluidized bed conversion of dimethyl ether to olefins.* Applied Catalysis A: General, 2008. **341**(1): p. 112-118.

74. Hirota, Y., et al., *Light olefins synthesis from methanol and dimethylether over SAPO-34 nanocrystals.* Catalysis letters, 2010. **140**(1-2): p. 22-26.

75. Ahmed, M.H., O. Muraza, and A.M. Al Amer, *Effect of synthesis parameters and ion exchange on crystallinity and morphology of EU-1 zeolite.* Journal of Alloys and Compounds, 2014.

76. Li, Q., et al., *Aging effects on the nucleation and crystallization kinetics of colloidal TPA-silicalite-1.* Microporous and mesoporous materials, 2001. **43**(1): p. 51-59.

77. Abdo, S.F., H. Abrevaya, and R.L. Patton, *Catalytic naphtha cracking catalyst and process.* 2005, Google Patents.

78. Zhang, X., D. Tang, and G. Jiang, *Synthesis of zeolite NaA at room temperature: The effect of synthesis parameters on crystal size and its size distribution.* Advanced Powder Technology, 2013. **24**(3): p. 689-696.

79. Jafari, M., et al., *Investigations on hydrothermal synthesis parameters in preparation of nanoparticles of LTA zeolite with the aid of TMAOH.* Powder Technology, 2013. **237**(0): p. 442-449.

80. Karimi, R., et al., *Studies of the effect of synthesis parameters on ZSM-5 nanocrystalline material during template-hydrothermal synthesis in the presence of chelating agent.* Powder Technology, 2012. **229**: p. 229-236.

81. Bayati, B., A.A. Babaluo, and R. Karimi, *Hydrothermal synthesis of nanostructure NaA zeolite: The effect of synthesis parameters on zeolite seed size and crystallinity.* Journal of the European Ceramic Society, 2008. **28**(14): p. 2653-2657.

82. Kumar, N., et al., *Effect of synthesis time and mode of stirring on physico-chemical and catalytic properties of ZSM-5 zeolite catalysts.* Applied Catalysis A: General, 2002. **235**(1): p. 113-123.

83. Konno, H., et al., *Kinetics of n-hexane cracking over ZSM-5 zeolites – Effect of crystal size on effectiveness factor and catalyst lifetime.* Chemical Engineering Journal, 2012. **207–208**(0): p. 490-496.

84. Fogler, H.S., *Elements of chemical reaction engineering.* 1999.

85. Bhatia, S., *Zeolite catalysts: principles and applications.* 1989: CRC press.

86. Peixoto, D., S. Cabral de Menezes, and M. Pais da Silva, *Influence of different processes of dealumination on acid properties of an H-ferrierite zeolite.* Materials Letters, 2003. **57**(24): p. 3933-3942.

87. Batonneau-Gener, I., et al., *Influence of steaming and acid-leaching treatments on the hydrophobicity of HBEA zeolite determined under static conditions.* Microporous and Mesoporous Materials, 2008. **110**(2): p. 480-487.

88. Boveri, M., et al., *Steam and acid dealumination of mordenite: characterization and influence on the catalytic performance in linear alkylbenzene synthesis.* Catalysis today, 2006. **114**(2): p. 217-225.

89. Martins, J., et al., *Sodium exchange over H-EU-1 zeolite. Part I: Physicochemical characterization.* Microporous and Mesoporous Materials, 2013. **171**(0): p. 230-237.

90. You, S.J. and E.D. Park, *Effects of dealumination and desilication of H-ZSM-5 on xylose dehydration.* Microporous and Mesoporous Materials, 2014. **186**: p. 121-129.

Vitae

Name	Mohamed Hassan Mohamed Ahmed
Nationality	Sudanese
Date of Birth	01/10/1989
Email	mohammed_alansari89@yahoo.com
Address	King Fad University – BLD812 – Room118
Academic Background	Chemical Engineering

Since I graduated from University of Khartoum, chemical engineering department September 2010 with first class degree (honor) I started work in scientific researches. I worked in a project of "Utilizing the solar energy for refrigeration" funded by University of Hamburg. Then, I applied to KFUPM master program in 2012 and I got a scholarship and a research assistant position in Center of Research Excellence in Nanotechnology. Since I joined the center I took excessive training in many characterization techniques used in the field of nanotechnology like (FTIR, BET, GC, UPLC, PSA, SEM and XRD). My thesis research was in the area of heterogeneous catalysis and how to develop an acid solid catalyst (Zeolite) with modified properties under the title of "Synthesis and characterization of hierarchal EU-1(EUO) zeolite and its application in converting DME to olefins".

Publications and conferences

1. Effect of synthesis parameters and ion exchange on crystallinity and morphology of EU-1 zeolite, M.H. Ahmed, O. Muraza, A.M. Al-Amer, Journal of Alloys and Compounds, 617 (2014) 408-412.
2. Poster accepted in UK Catalysis Conference Jan 2015.
3. Development of desilicated EU-1 zeolite and its application in conversion of dimethyl ether to olefins, Microporous and Mesoporous Materials (IF 3.3)(Submitted).
4. Development of hierarchical EU-1 zeolite by sequential acid and alkaline treatments for selective dimethyl ether to propylene (DTP) reaction, Applied Catalysis A: General (IF 4) (Submitted).